SEARCH FOR SOLAR AXIONS IN THE CAST EXPERIMENT USING THE MICROMEGAS DETECTOR

PhD THESIS

Konstantinos Kousouris

Outline

I. Theory

The strong CP problem, the dynamic Peccei–Quinn solution, axion and its properties, axion–photon oscillation.

II. CAST

Solar axions, principle of the experiment, the magnet and the detectors.

III. Micromegas

General description and properties, the micromegas of CAST, typical performance.

IV. Analysis & Results

Simulation, 2003 data, 2004 data.

THEORY

The Strong CP Problem

$$\tilde{\vec{G}}_{\mu\nu} = \frac{1}{2}\varepsilon_{\mu\nu\alpha\beta}\vec{G}^{\alpha\beta}$$

$$L_{\bar{\theta}} = \frac{g_s^2\bar{\theta}}{32\pi^2}\vec{G}^{\mu\nu}\cdot\tilde{\vec{G}}_{\mu\nu}$$

$$\vec{G}^{\mu\nu}\cdot\tilde{\vec{G}}_{\mu\nu} \qquad \partial^\mu K_\mu$$

$$K_\mu = 2\varepsilon_{\mu\alpha\beta\gamma}\vec{A}^\alpha\cdot\left\{\partial^\beta\vec{A}^\gamma + \frac{g_s}{3}\left(\vec{A}^\beta\times\vec{A}^\gamma\right)\right\}$$

$$|\theta\rangle = \sum_n e^{in\theta}|n\rangle$$

$$\bar{\theta} = \theta + \mathrm{Arg}(\det(M_q))$$

Neutron electric dipole moment

$$\left.\begin{array}{l} d_n^{theory} \approx \bar{\theta}\times 10^{-15}\,e\cdot cm \\ d_n^{exp} < 0.63\times 10^{-25}\,e\cdot cm \end{array}\right\} \Rightarrow \bar{\theta} \sim 10^{-10}$$

Why so small;

The Standard Model <u>DOES NOT</u> provide an answer.

Extra term in the QCD Lagrangian:

α. CP violating.

β. Total divergence (Bardeen current).

γ. Not affecting the perturbative behavior of the theory.

δ. Non zero contribution (vacuum topology).

The Peccei-Quinn mechanism

PQ Symmetry: global, axial, beyond the Standard Model.

Spontaneous symmetry breaking at scale f_α

Axion: Goldstone boson, pseudoscalar, neutral.

$$L_\alpha = C\frac{g_s^2}{32\pi^2 f_\alpha}\alpha(x)\vec{G}^{\mu\nu}\cdot\vec{\tilde{G}}_{\mu\nu}$$

$$V_{eff}(\alpha) = \frac{1}{2}K\left(\bar{\theta} + C\frac{\alpha(x)}{f_\alpha}\right)^2$$

$$\langle\alpha\rangle = -\frac{f_\alpha\bar{\theta}}{C}$$

$$m_\alpha^2 = \left(\frac{\partial^2 V_{eff}}{\partial^2\alpha}\right)_{\langle\alpha\rangle}$$

The vacuum expectation value of the axion field eliminates the QCD term at the cost of axion appearance.

Axion models

PQWW

- $f_\alpha = f_{ew}$
- Two Higgs fields.
- Fermions: PQ charge.

DFSZ

- $f_\alpha >> f_{ew}$
- Two Higgs fields and one scalar field.
- Fermions: PQ charge.

KSVZ

- $f_\alpha >> f_{ew}$
- One Higgs field, one scalar field, one exotic quark with PQ charge.

Experimentally excluded.

$$\Phi'_u = e^{i\alpha\Gamma_u}\Phi_u \ , \ \Phi'_d = e^{i\alpha\Gamma_d}\Phi_d$$

$$u'_L = e^{\frac{1}{2}i\alpha\Gamma_u}u_L \ , \ u'_R = e^{-\frac{1}{2}i\alpha\Gamma_u}u_R$$

$$d'_L = e^{\frac{1}{2}i\alpha\Gamma_d}d_L \ , \ d'_R = e^{-\frac{1}{2}i\alpha\Gamma_d}d_R$$

$$\Phi'_u = e^{i\alpha X_u}\Phi_u \ , \ \Phi'_d = e^{i\alpha X_d}\Phi_d$$

$$\sigma' = e^{i\alpha X_\sigma}\sigma \ , \ X_u + X_d = -2X_\sigma = 1$$

$$u'_L = e^{\frac{1}{2}i\alpha X_u}u_L \ , \ u'_R = e^{-\frac{1}{2}i\alpha X_u}u_R$$

$$d'_L = e^{\frac{1}{2}i\alpha X_d}d_L \ , \ d'_R = e^{-\frac{1}{2}i\alpha X_d}d_R$$

$$\psi'_L = e^{\frac{1}{2}i\alpha}\psi_L \ , \ \psi'_R = e^{-\frac{1}{2}i\alpha}\psi_R$$

$$\sigma' = e^{i\alpha}\sigma$$

Hadronic axion

Properties

Electromagnetic interaction

$$L_\alpha = \frac{1}{4} g_{\alpha\gamma\gamma} \alpha F^{\mu\nu} \tilde{F}_{\mu\nu}$$

$$g_{\alpha\gamma\gamma} = C \frac{e^2}{2\pi^2 f_\alpha}$$

$$C = \sum_{\text{fermions}} Q_{em}^2 Q_{PQ}$$

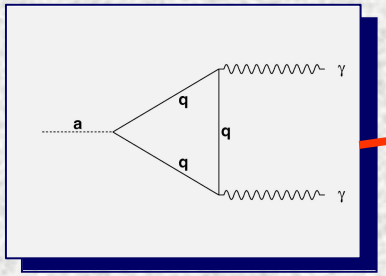

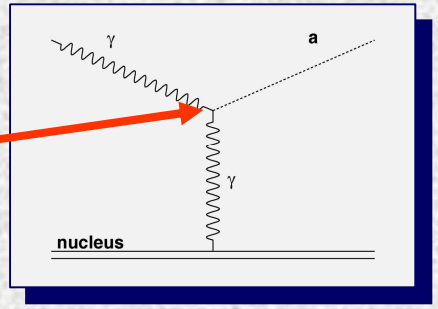

Primakoff effect

$$\frac{d\sigma_{\alpha\leftrightarrow\gamma}}{d\Omega} = \frac{g_{\alpha\gamma\gamma}^2 Z^2 e^2}{32\pi^2} \frac{\left|\vec{p}_\alpha \times \vec{p}_\gamma\right|^2}{\left|\vec{p}_\alpha - \vec{p}_\gamma\right|^4}$$

Axion–Photon conversion in the Coulomb field of a nucleus.

Axion lifetime

$$\tau(\alpha \to \gamma\gamma) \sim \frac{10^{23}}{\left[m_\alpha(\text{eV})\right]^5} \text{sec}$$

Axion mass

$$m_\alpha = N_g m_\pi \cdot \frac{f_\pi}{f_\alpha} \cdot \frac{\sqrt{m_u m_d}}{m_u + m_d}$$

Number of quark generations carrying PQ charge.

$f_\alpha >> 1$GeV

Invisible Axion

Axion – Photon oscillation

Assumptions

- vacuum,
- weak interaction: $g_{\alpha\gamma\gamma} << \frac{m_\alpha^2}{BE}$
- transverse magnetic field: $\vec{p}_\alpha \perp \vec{B}$
- relativistic limit: $E >> m_\alpha$

$$L = -\frac{1}{4}F_{\mu\nu}F^{\mu\nu} + \frac{1}{2}\left(\partial_\mu\alpha\partial^\mu\alpha - m_\alpha^2\alpha^2\right) + \frac{1}{4}g_{\alpha\gamma\gamma}\alpha F_{\mu\nu}\tilde{F}^{\mu\nu}$$

$$\left(\nabla^2 + m_\alpha^2\right)\alpha - g_{\alpha\gamma\gamma}\frac{\partial\vec{A}}{\partial t}\cdot\vec{B} = 0$$

$$\nabla^2\vec{A} + g_{\alpha\gamma\gamma}\frac{\partial\alpha}{\partial t}\vec{B} = \vec{0}$$

$$F_{\mu\nu} = F_{\mu\nu}^{ext} + \partial_\mu A_\nu - \partial_\nu A_\mu$$

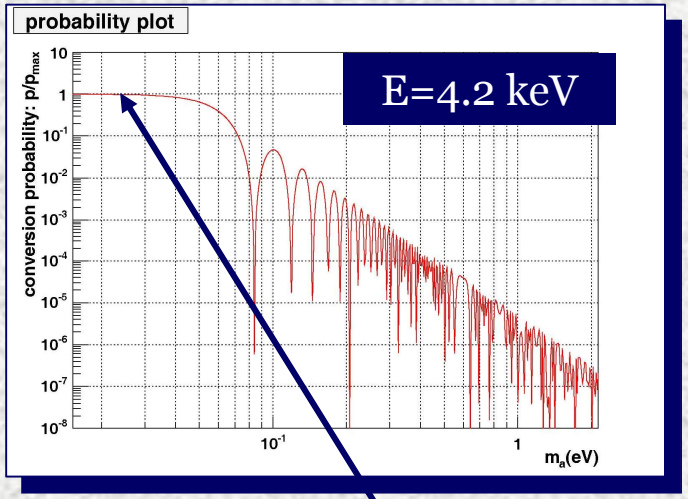

$$P_{\alpha\to\gamma}(z) = \frac{B^2 g_{\alpha\gamma\gamma}^2}{q^2}\sin^2\left(\frac{qz}{2}\right) \xrightarrow{q\to 0} \frac{1}{4}B^2 g_{\alpha\gamma\gamma}^2 z^2$$

$$q = \frac{m_\alpha^2}{2E}$$ (vacuum momentum transfer)

CAST

Cern Axion Solar Telescope

Solar Axions

Assumptions

- Hadronic Axions.
- Primakoff Effect.
- Charge screening.
- Standard Solar Model.

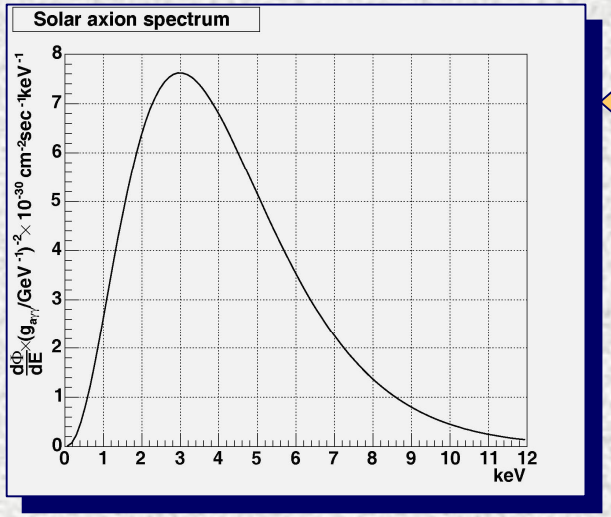

Axion spectrum on Earth

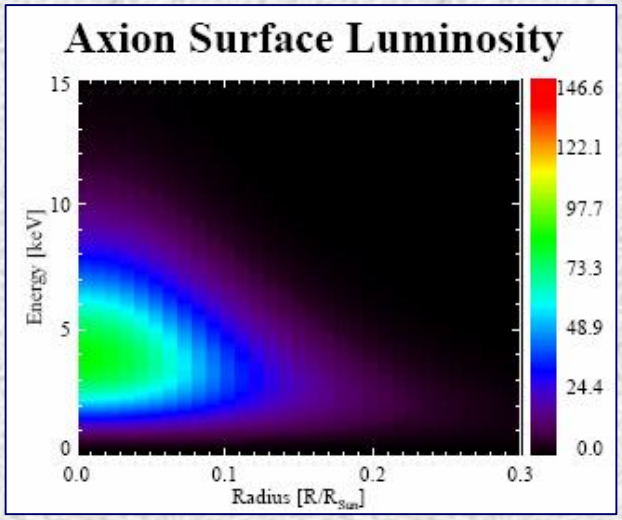

$$\frac{d\Phi_\alpha}{dE} = 6.02\times10^{10}\cdot g_{10}^2\cdot E^{2.481}\cdot e^{-E/1.205}\ cm^{-2}s^{-1}keV^{-1}$$

$$L_\alpha = 1.85\times10^{-3}\cdot g_{10}^2\cdot L_\odot$$

$$\langle E_\alpha\rangle = 4.2\ keV$$

$$\Phi_\alpha \quad 3.67\times10^{11}\cdot g_{10}^2\cdot cm^{-2}s^{-1}$$

$$g_{10} = g_{\alpha\gamma\gamma}\times\left(10^{10}GeV\right)$$

Detection Principle

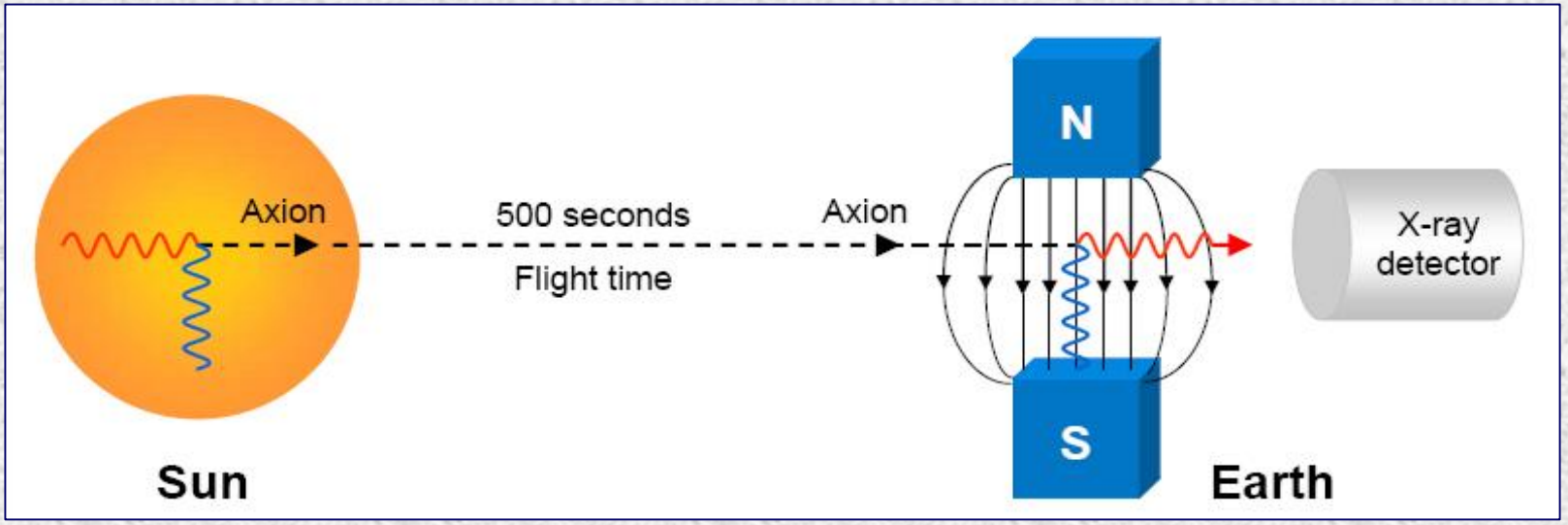

Axions are produced in the Solar core through the Primakoff effect and travel freely to the Earth where they are converted to photons, interacting with a transverse magnetic field which can align to the Sun (Helioscope). If there is an excess of photons when tracking the Sun, it is an indication of axion existence.

Experimental apparatus

- Prototype, dipole LHC magnet.
- Superconducting: T=1.8K, I=13,000A.
- B=9T, L=9.26m.
- ±8° vertical motion, 80° horizontal motion.
- 3h Sun tracking daily.

Phase I: pipes in vacuum.

Phase II: pipes filed with gas (He3, He4).

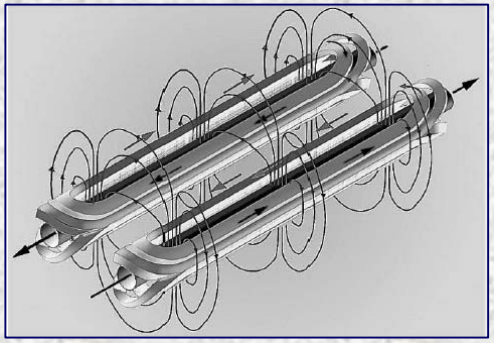

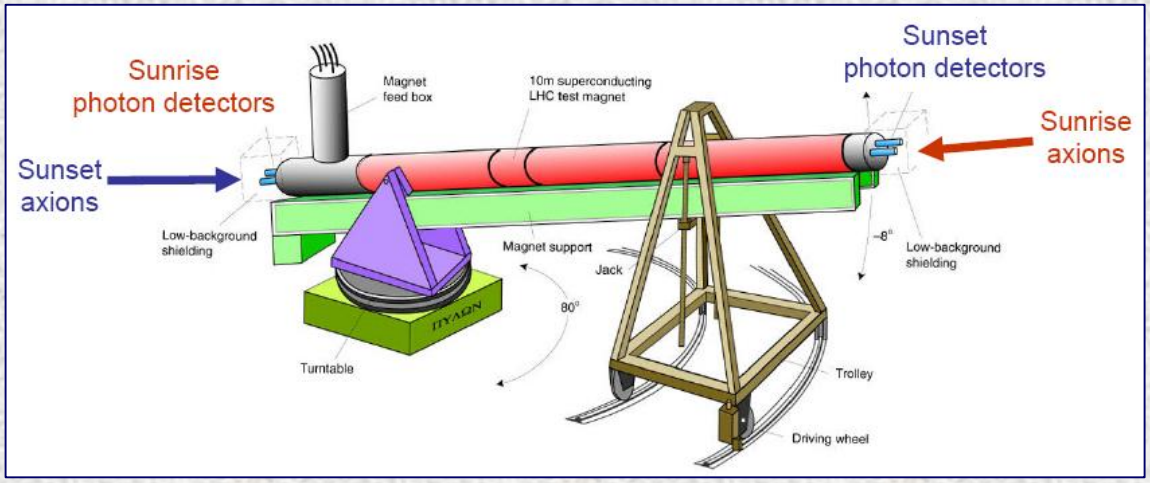

Detectors

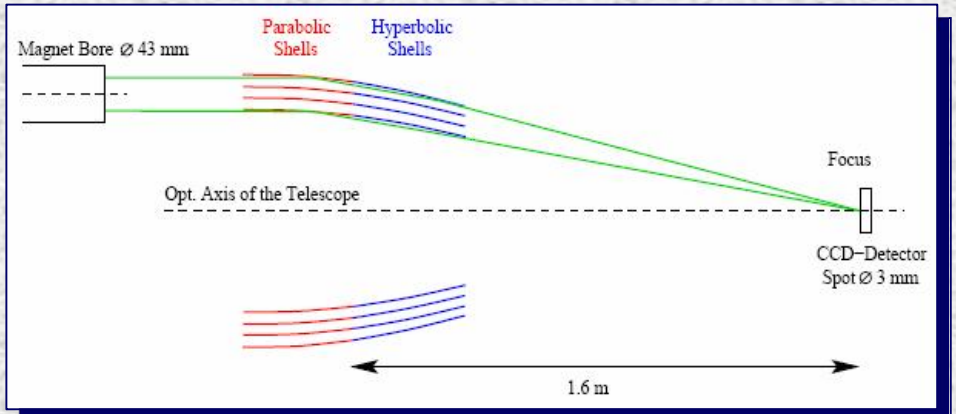

Telescope and CCD

- Wolter I optical device, prototype of ABRIXAS space mission. 27 coaxial gold-plated shells from Ni. Axionic image of the Sun.
- Charged Coupled Device (silicon detector). Pixel size: 150 x 150 μm².
- Spot: 3mm diameter, huge increase of CAST sensitivity.
- Covers one magnet bore and tracks the Sun during sunrise.

TPC

- Time Projection Chamber: conventional gas detector with 48 anode wires and 96 cathode wires, 3mm apart.
- Shielded. Constructed by Zaragoza University.
- Covers two magnet bores and tracks the Sun during sunset.

MICROMEGAS

- New technology, parallel plate gas detector with microstructure and spatial sensitivity.
- Constructed by Saclay and NCSR "Demokritos".
- Covers one magnet bore and tracks the Sun during sunrise.

Axionic parametric space

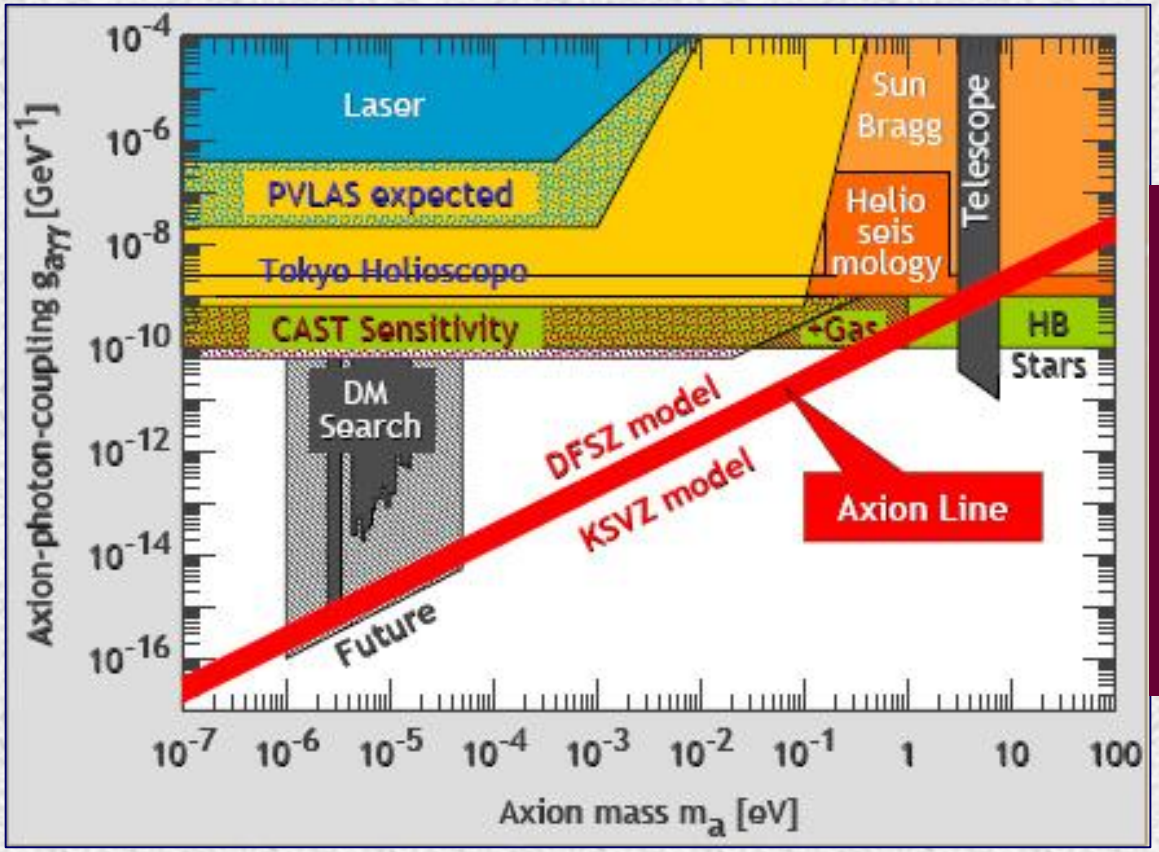

Sources

- Helioscopes.
- Laser experiments.
- Coherent Bragg scattering in crystals.
- Astrophysical arguments.
- Cosmological arguments.
- Dark matter experiments.

MICROMEGAS

Operation principle

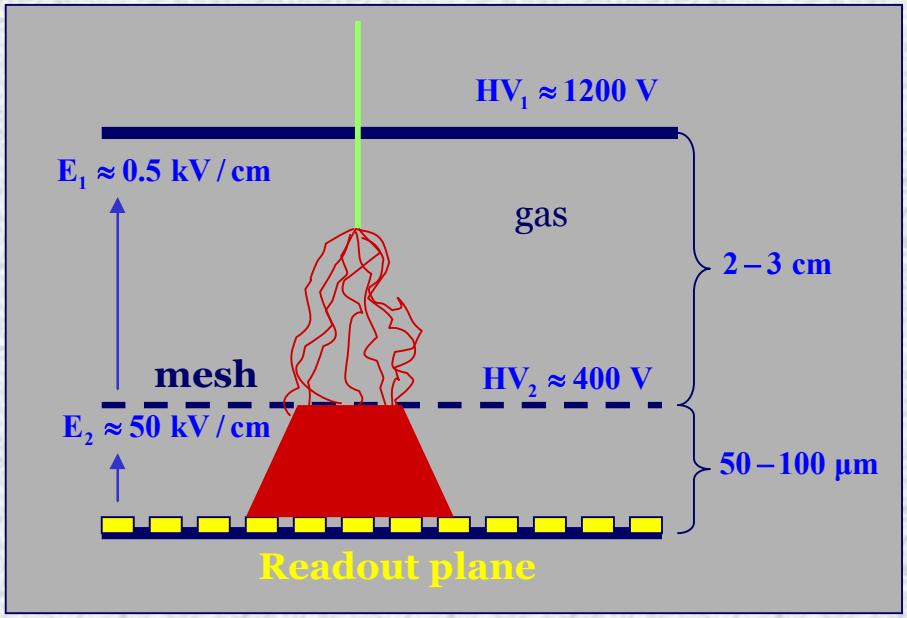

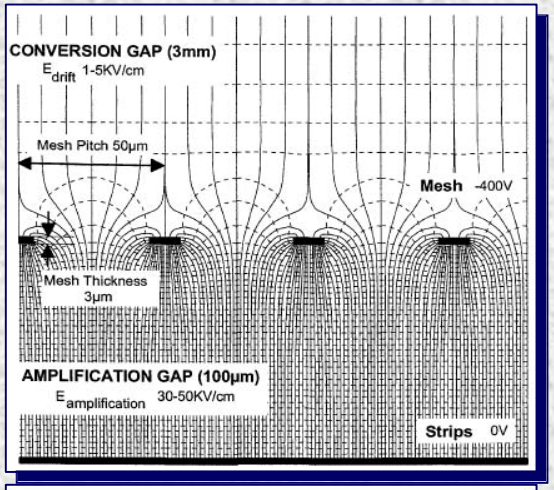

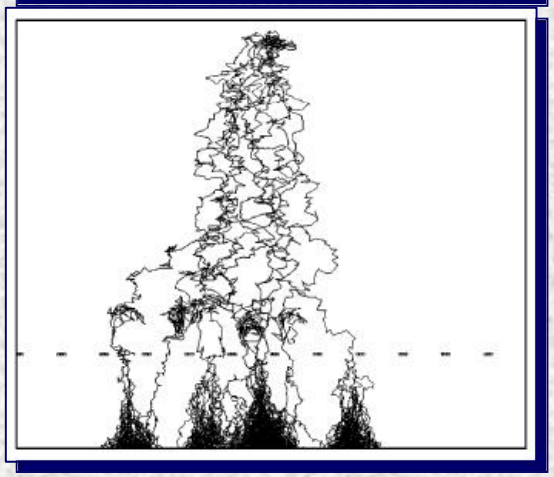

The Micromegas of CAST

Specifications

1. X-ray detection capability (energy 1-10 keV).
2. Typical energy resolution (20% at 5.9 keV).
3. Good efficiency.
4. Spatial sensitivity ~ 1 mm.
5. Calibration rate: 50Hz, data rate: 1Hz.

Ar (95%) + Isobutane (5%)

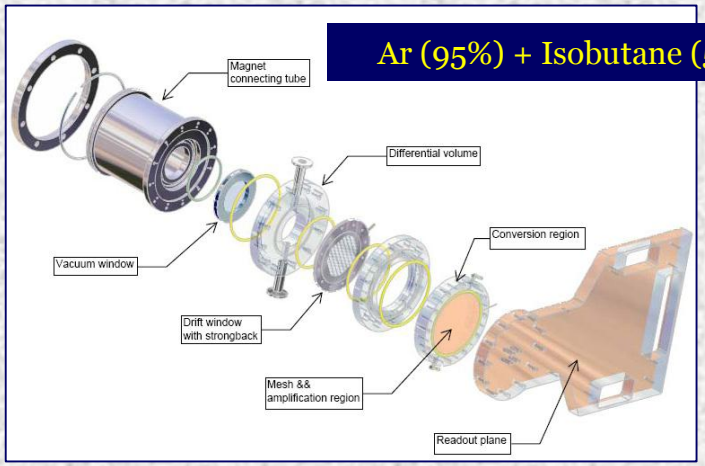

mesh

hole diameter: 25μm

pitch: 50μm

Two dimensional X-Y readout plane: 192 copper strips in each direction with 350μm pitch.

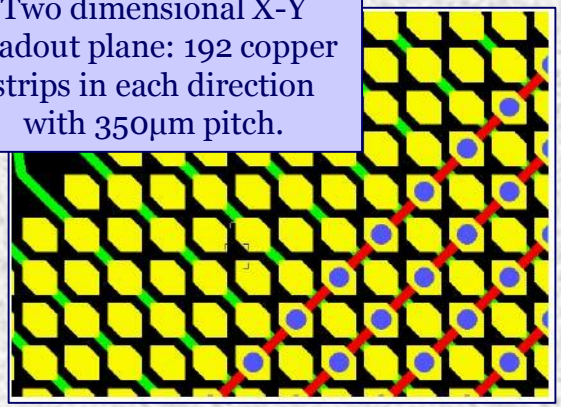

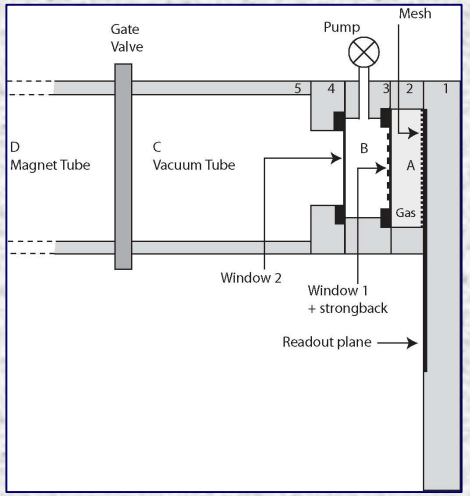

Electronics

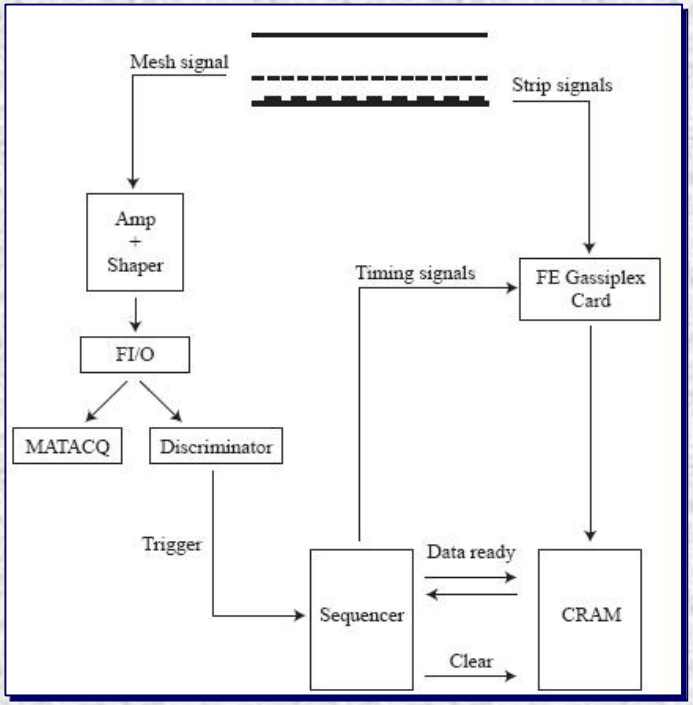

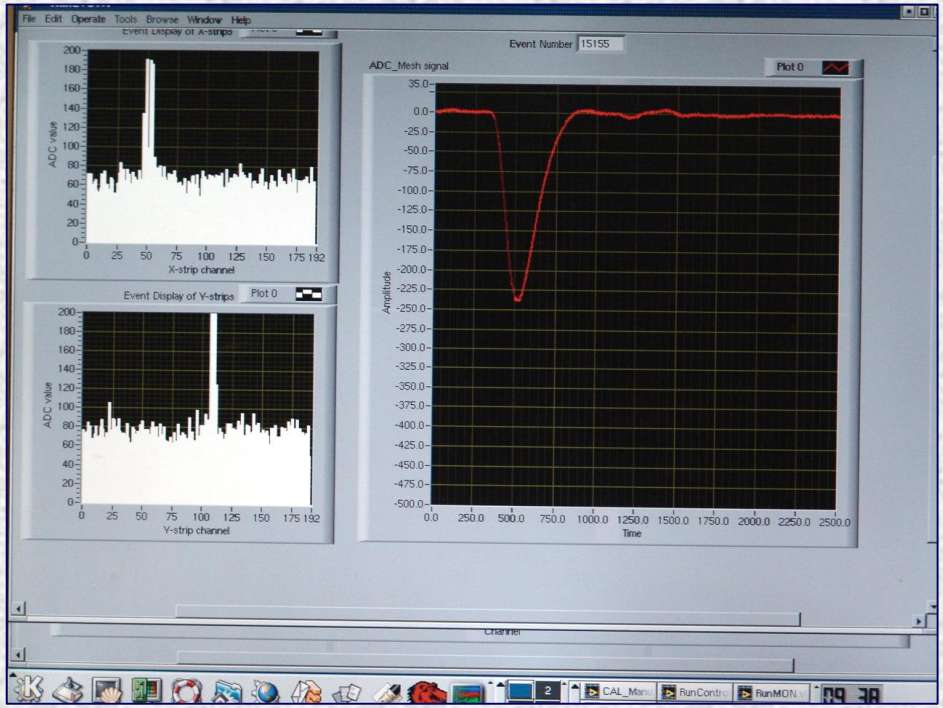

Data Acquisition System (DAQ)

Written in LabView (Linux+Windows), developed in NCSR "Demokritos" (T. Geralis, G. Fanourakis).

Operation: **Non Paralyzable**. Dead time: **14 msec**.

Characterization

Absolute efficiency

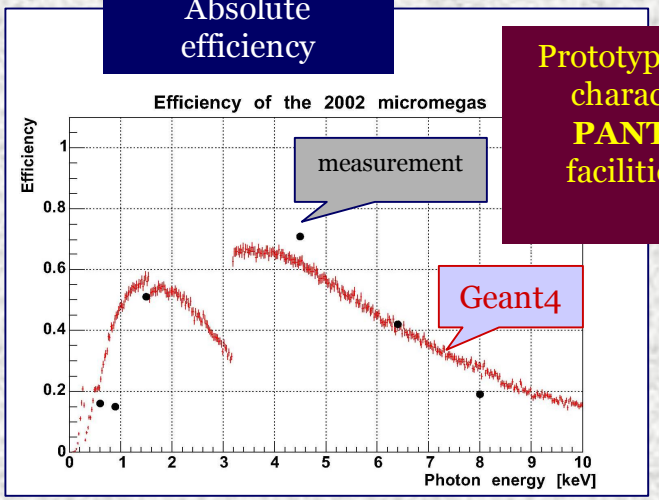

Prototype Micromegas: characterization at **PANTHER**, MPE facilities – Munich, 2002.

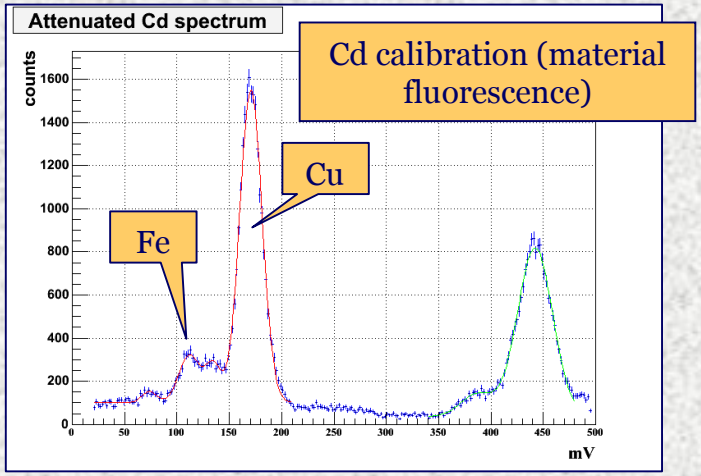

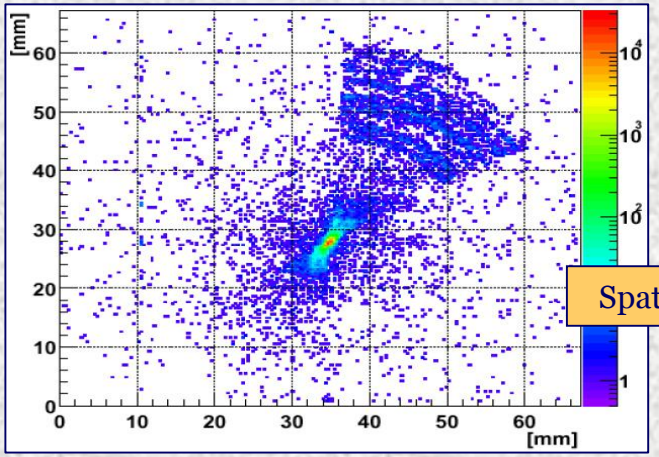

Linearity check

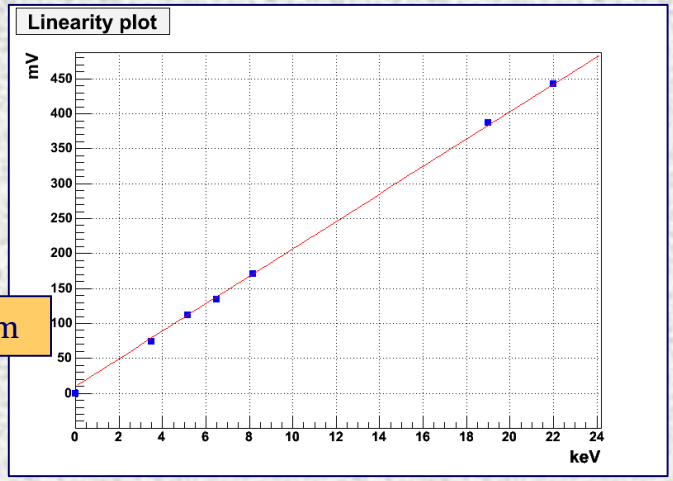

Spatial sensitivity: ~0.1 mm

ANALYSIS & RESULTS

Simulation (introduction)

Description

- GEANT4 toolkit.
- Exact reconstruction of the detector's geometry and materials.
- Goals:
  1. Calculation of the detector efficiency for photons hitting transversely the side facing the magnet bore.
  2. Influence of gas density variation in the detector.
  3. Qualitative reproduction of the measured background.
- The simulation takes into account the energy deposition in the detector and NOT the full event reconstruction through the whole detection chain.

Simulation (efficiency)

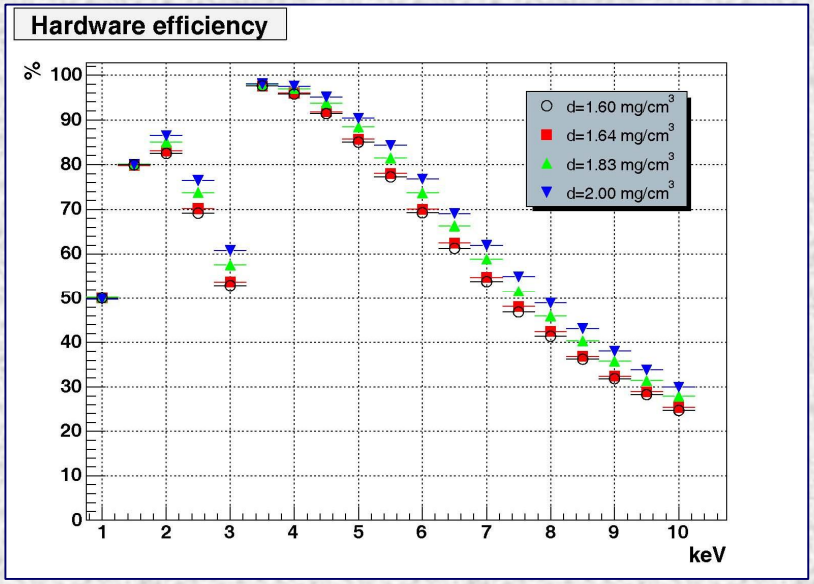

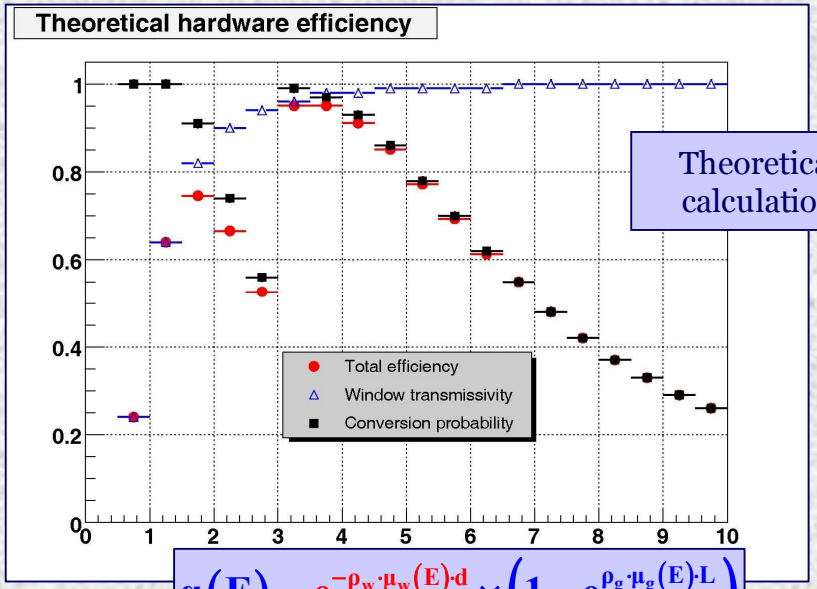

Theoretical calculation

$$\alpha(E) = e^{-\rho_w \cdot \mu_w(E) \cdot d} \times \left(1 - e^{\rho_g \cdot \mu_g(E) \cdot L}\right)$$

windows

gas

Full agreement between simulation and theoretical calculation.

Simulation (background)

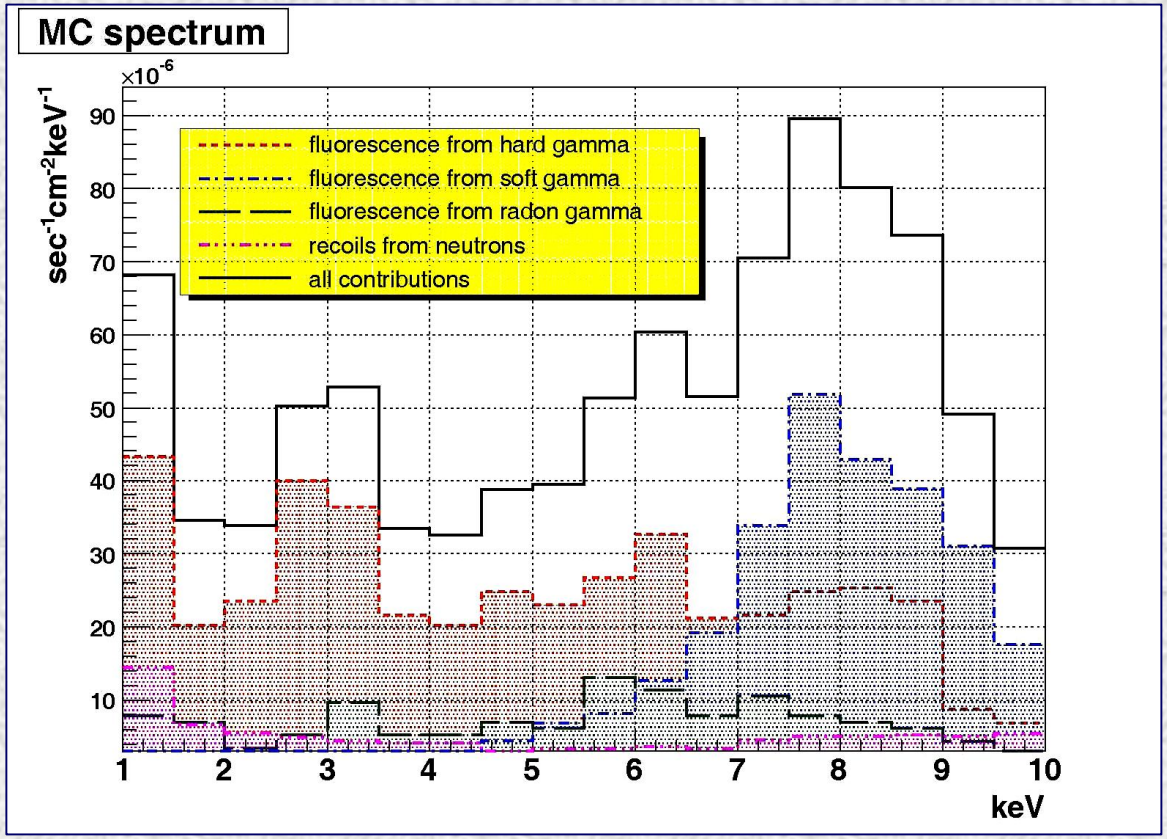

- Photons and neutrons of various energies are thrown to the detector isotropically.
- Event counting by local energy deposition.
- Normalization is arbitrary (based on the reconstruction of the Cu peak).
- Energy resolution is determined by the calibration measurements:

$$\delta \sqrt{\frac{6(\mathrm{keV})}{E}} \times 20\%$$

The background spectrum is determined by the fluorescence of the detector's building materials.

2003 - Calibration

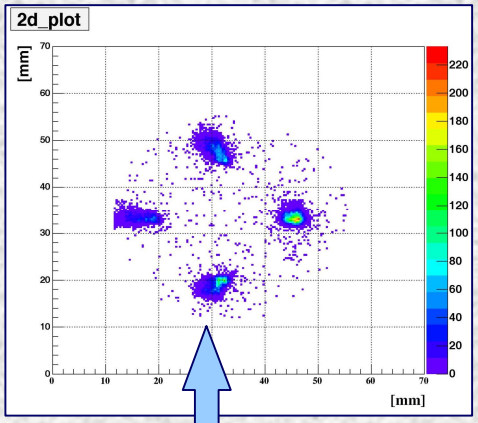

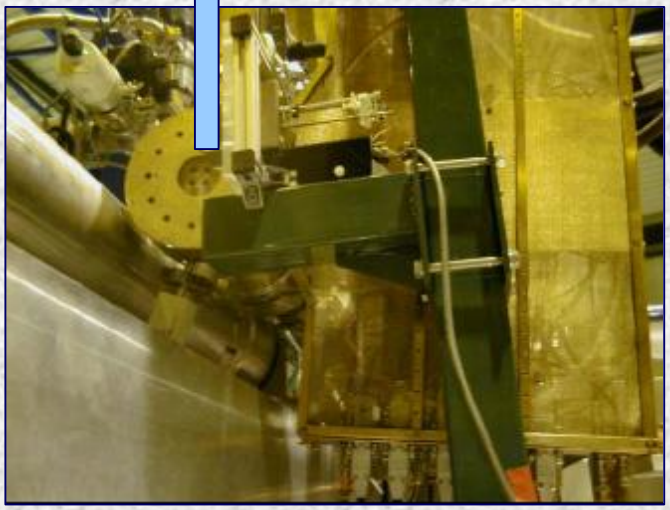

Prototype Micromegas **V3**

Conversion gap: 18 mm

Amplification gap: 50 μm

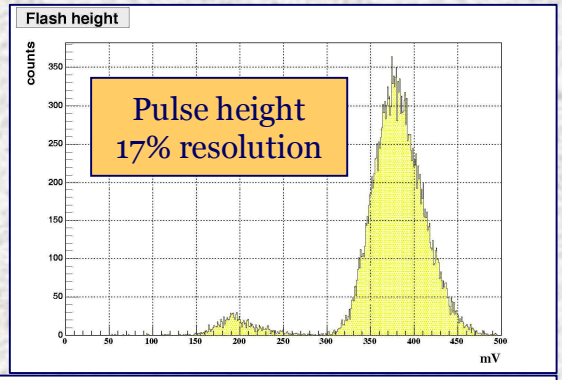

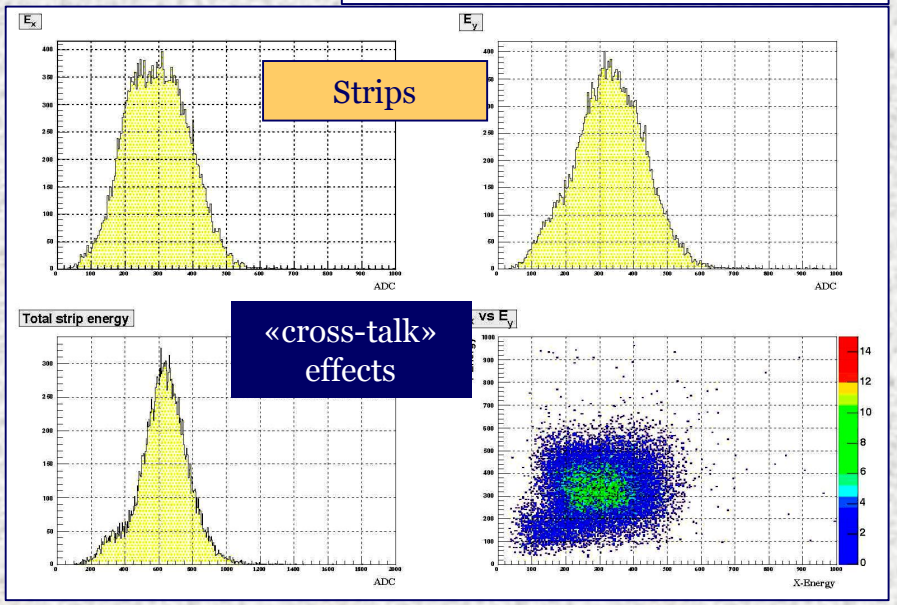

2003 - Data

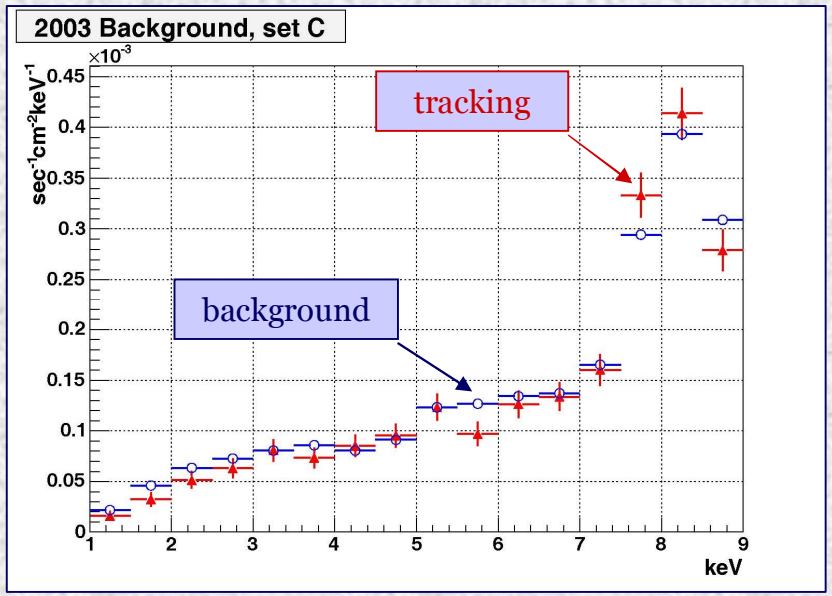

Event selection criteria

1. Single cluster.
2. Fiducial cut: circle with area A = 15.2 cm². Magnet bore = 14.5 cm².
3. Pulse risetime, width and ratio height/integral at most 2 standard deviations from the mean value.

Three different datasets due to different timing of the pulses.

SET	Tracking time (h)	Background time (h)	r_t $10^{-5}s^{-1}cm^{-2}keV^{-1}$	r_b $10^{-5}s^{-1}cm^{-2}keV^{-1}$	Energy range (keV)
A	56.5	592	8.4 ± 0.2	8.73 ± 0.06	1 - 7.5
B	11.6	143	10.7 ± 0.5	11.35 ± 0.14	1 – 8.0
C	24.9	477	13.5 ± 0.3	13.91 ± 0.08	1 – 9.0

2004 - Calibration

Prototype Micromegas **V4**

Conversion gap: 23.5 mm

Amplification gap: 100 μm

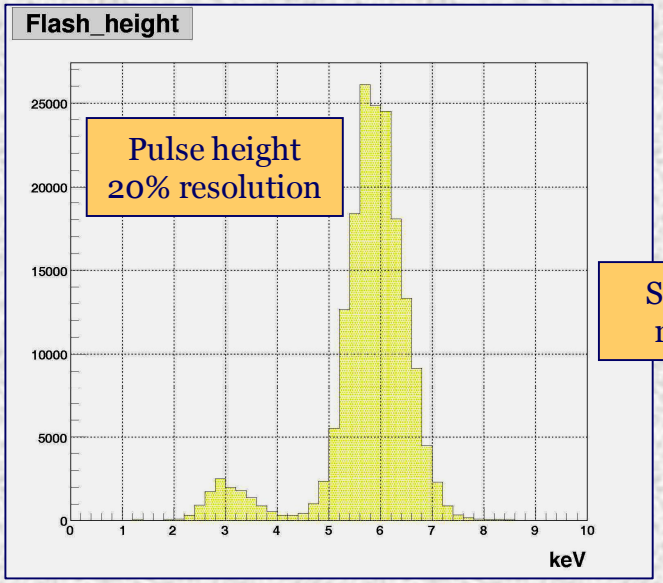

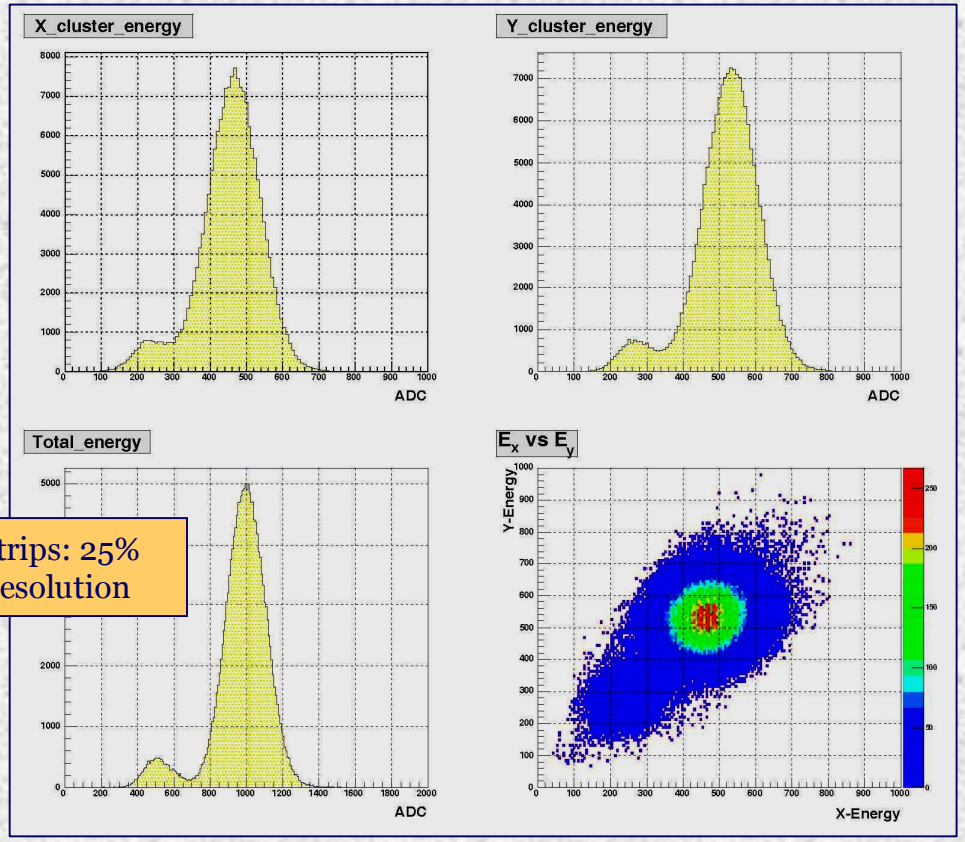

Strips: 25% resolution

Multivariate analysis (general)

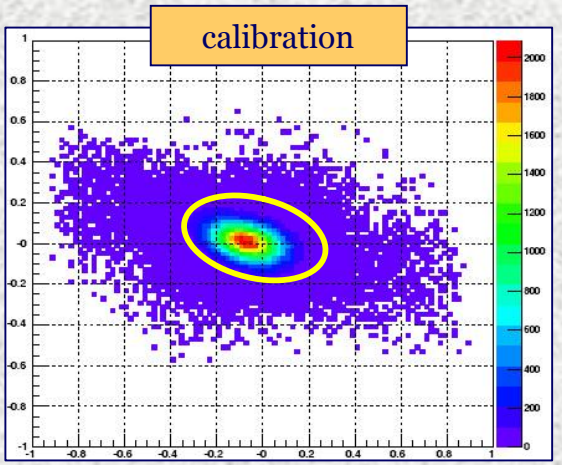

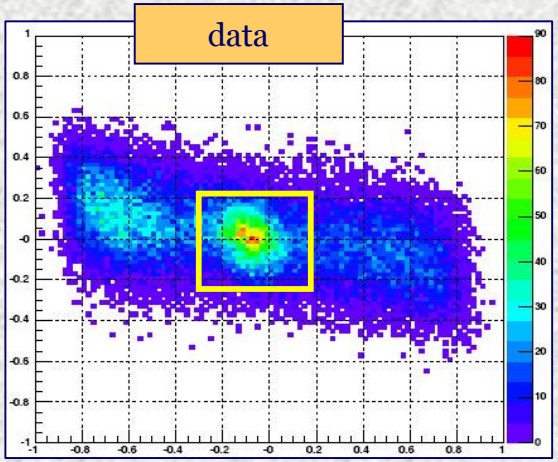

Goal:

Maximum efficiency and purity.

N variables x_i with mean values μ_i following Gaussian distibutions.

discriminant quantity

$$q = \sum_{ij} (x_i - \mu_i) V_{ij}^{-1} (x_j - \mu_j)$$

Covariance matrix

$$V_{ij} = \langle (x_i - \mu_i)(x_j - \mu_j) \rangle$$

χ^2_N distribution

$$f_N(q) = \frac{1}{2^{N/2}\Gamma(N/2)} \cdot q^{N/2-1} \cdot e^{-q/2}$$

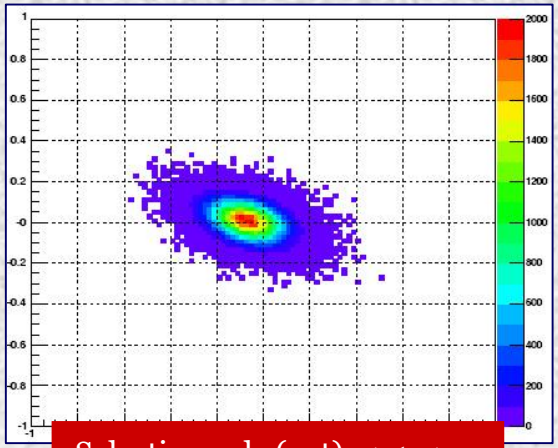

Selection rule (cut): $q < q_{max}$

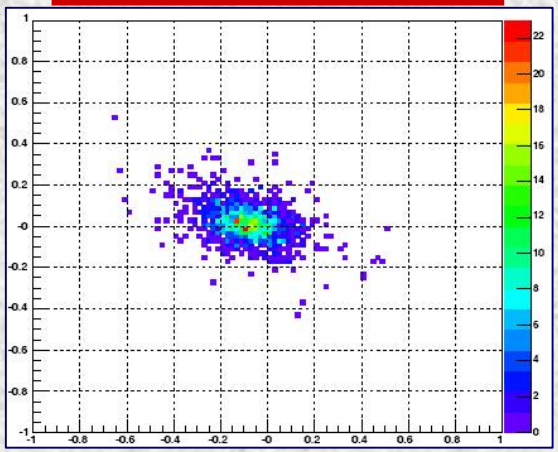

Multivariate analysis (discriminant quantities)

calibration

$x_1 = \text{risetime}$

$x_2 = \text{width}$

$$x_3 = \frac{e_x - e_y}{e_x + e_y} \quad \text{(charge assymetry)}$$

$$x_4 = \frac{\sigma_y m_x - \sigma_x m_y}{\sigma_y m_x + \sigma_x m_y} \quad \text{(multiplicity assymetry)}$$

$$x_5 = \frac{I}{10^3 H} \quad \text{(height-integral correlation)}$$

$$x_6 = \frac{I}{10^3 \left(e_x + e_y\right)} \quad \text{(pulse-strip correlation)}$$

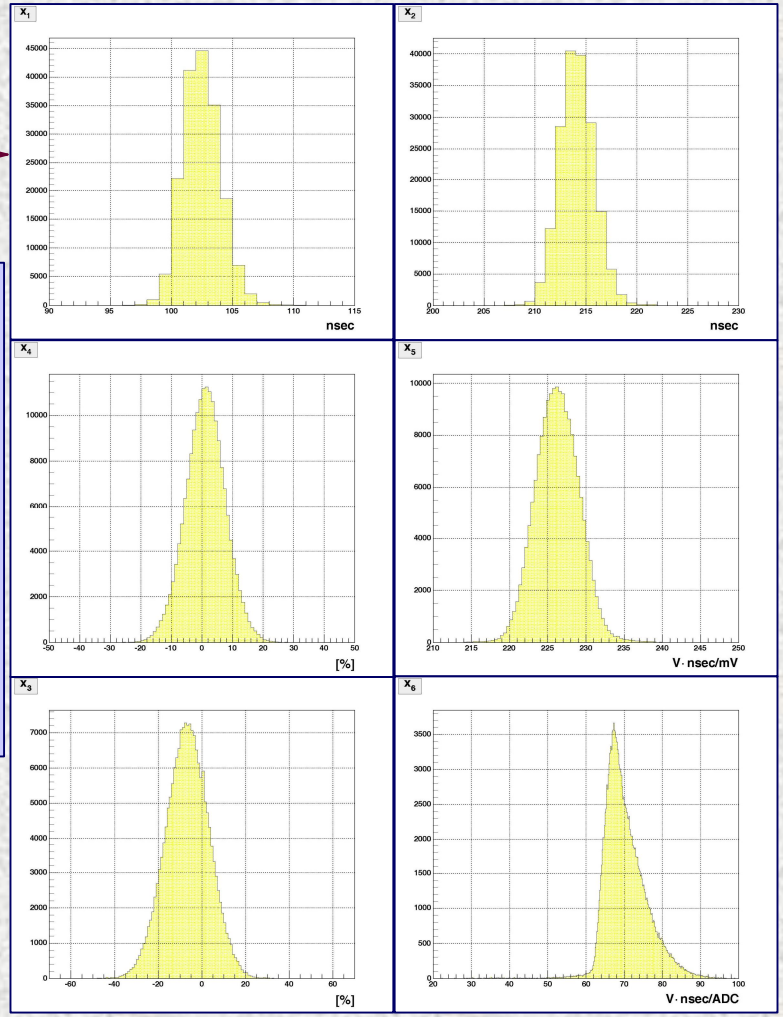

Multivariate analysis (calibration)

$$\left.\begin{array}{l}\mu_i(E)=\text{const.}\\ \sigma_i(E)\sim E^{-3/4}\end{array}\right\}\Rightarrow V_{ij}^{-1}(E)=\left(\frac{E}{E_o}\right)^{3/2}V_{ij}^{-1}(Eo)$$

$$\tilde{q}=\left(\frac{E_o}{E}\right)^{3/2}\times\sum_{ij}(x_i-\mu_i)\cdot V_{ij}^{-1}(E_o)\cdot(x_i-\mu_i)$$

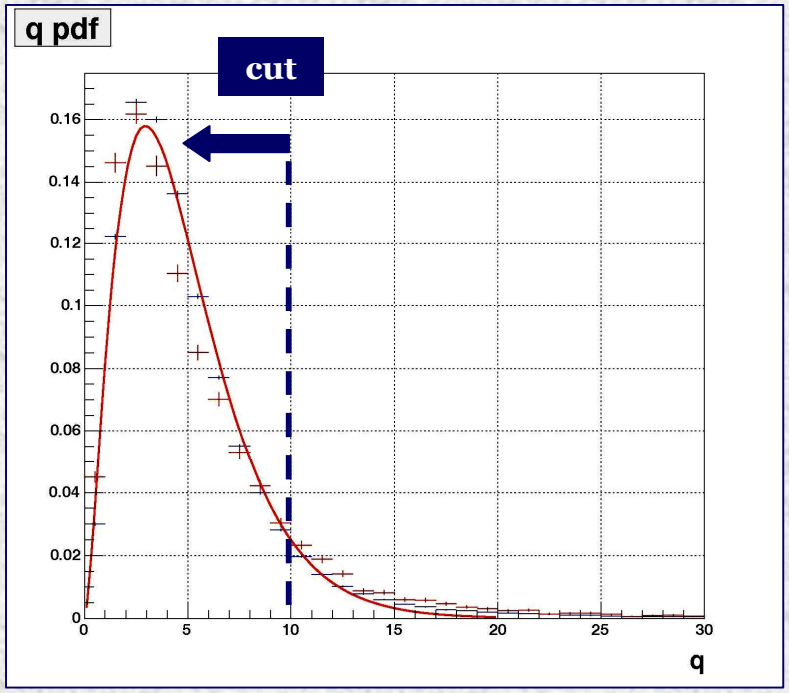

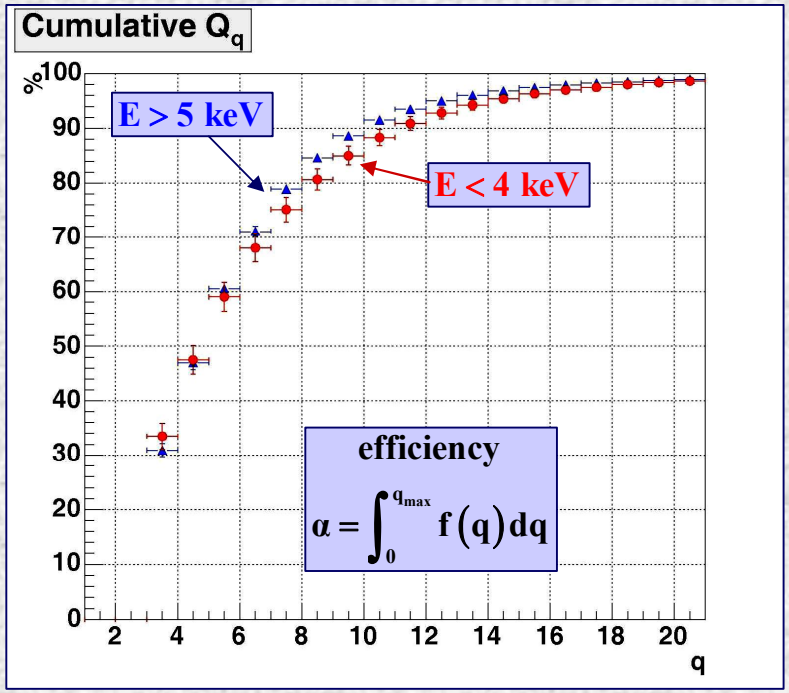

Multivariate analysis (data)

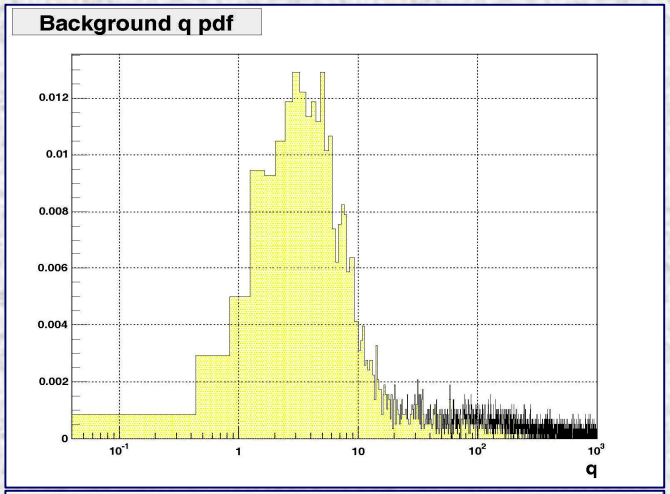

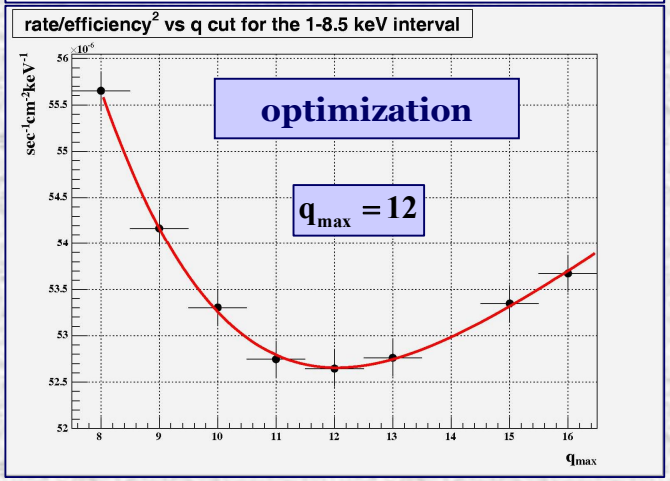

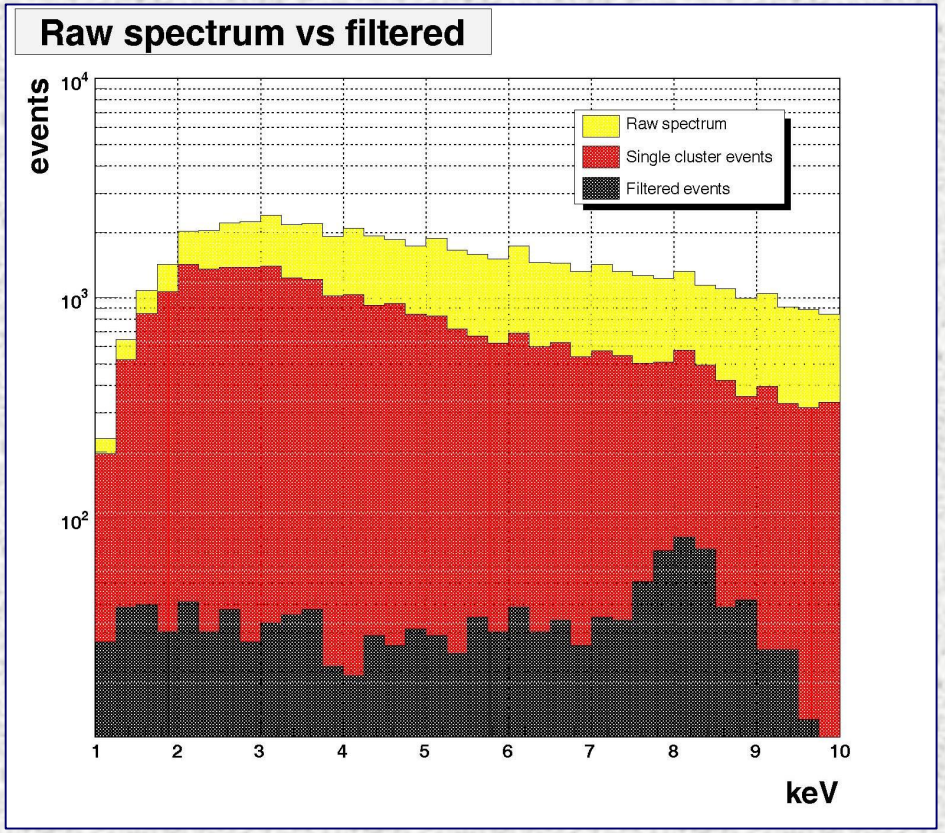

Background study

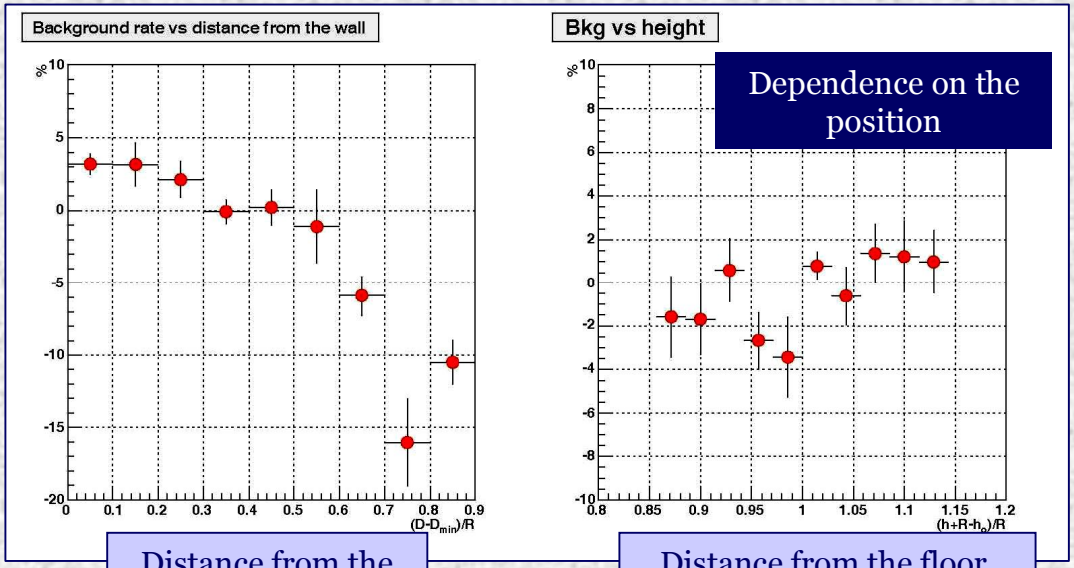

Distance from the closest wall.

Distance from the floor.

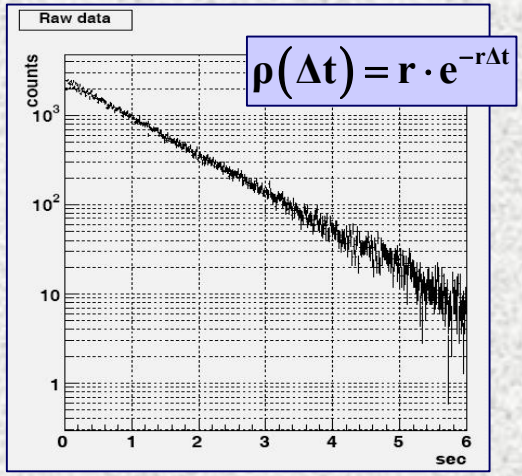

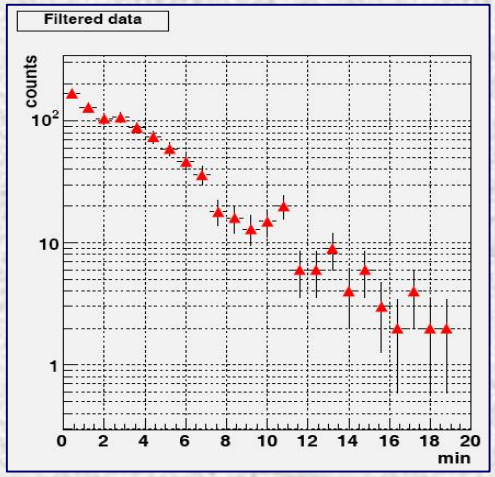

- ΔE = 1 – 8.5 keV.
- A = 15.2 cm².
- integration time: > 3000 h.
- trigger rate: ~ 1 Hz.
- filtered rate: ~ 18 events/h.
- cut efficiency: 92%.

Daily variation

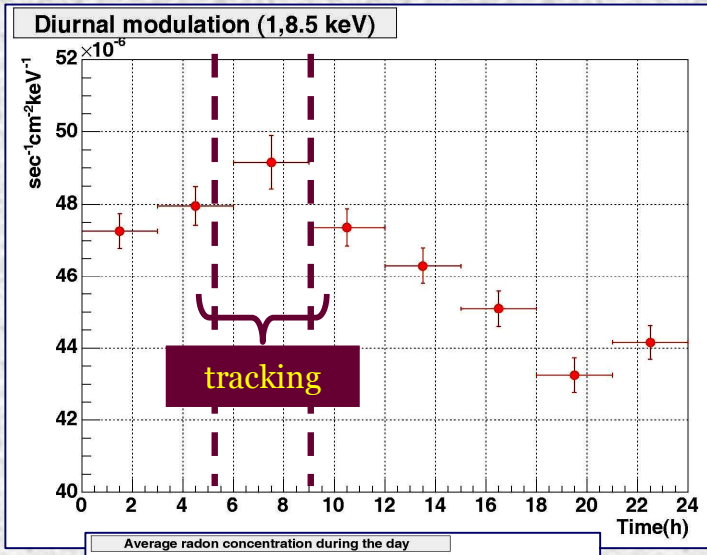

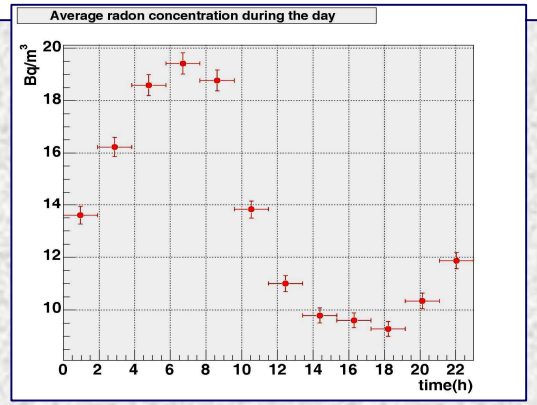

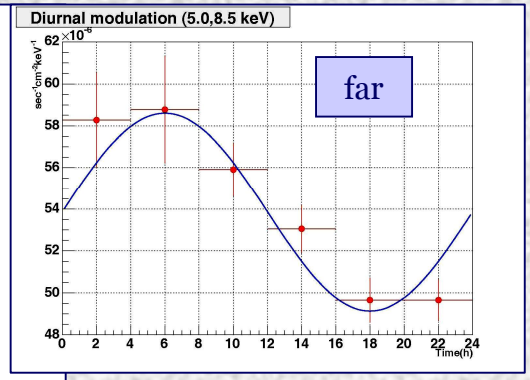

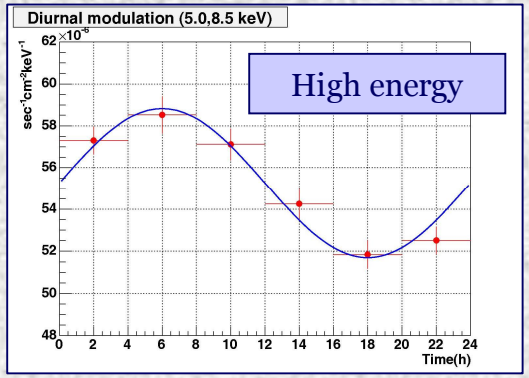

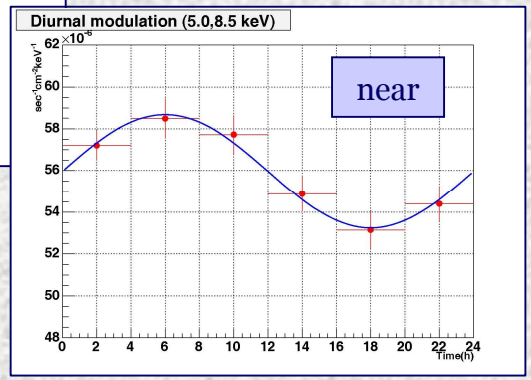

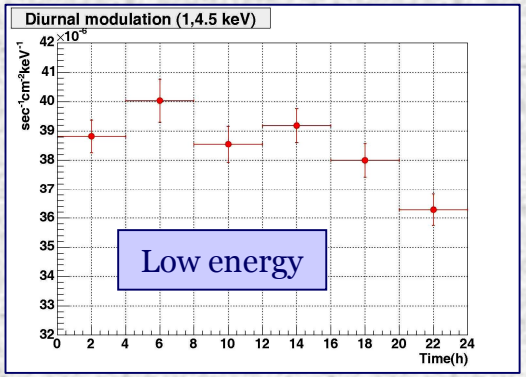

Clear daily variation, probably due to the variation of the Rn concentration.

Solar data

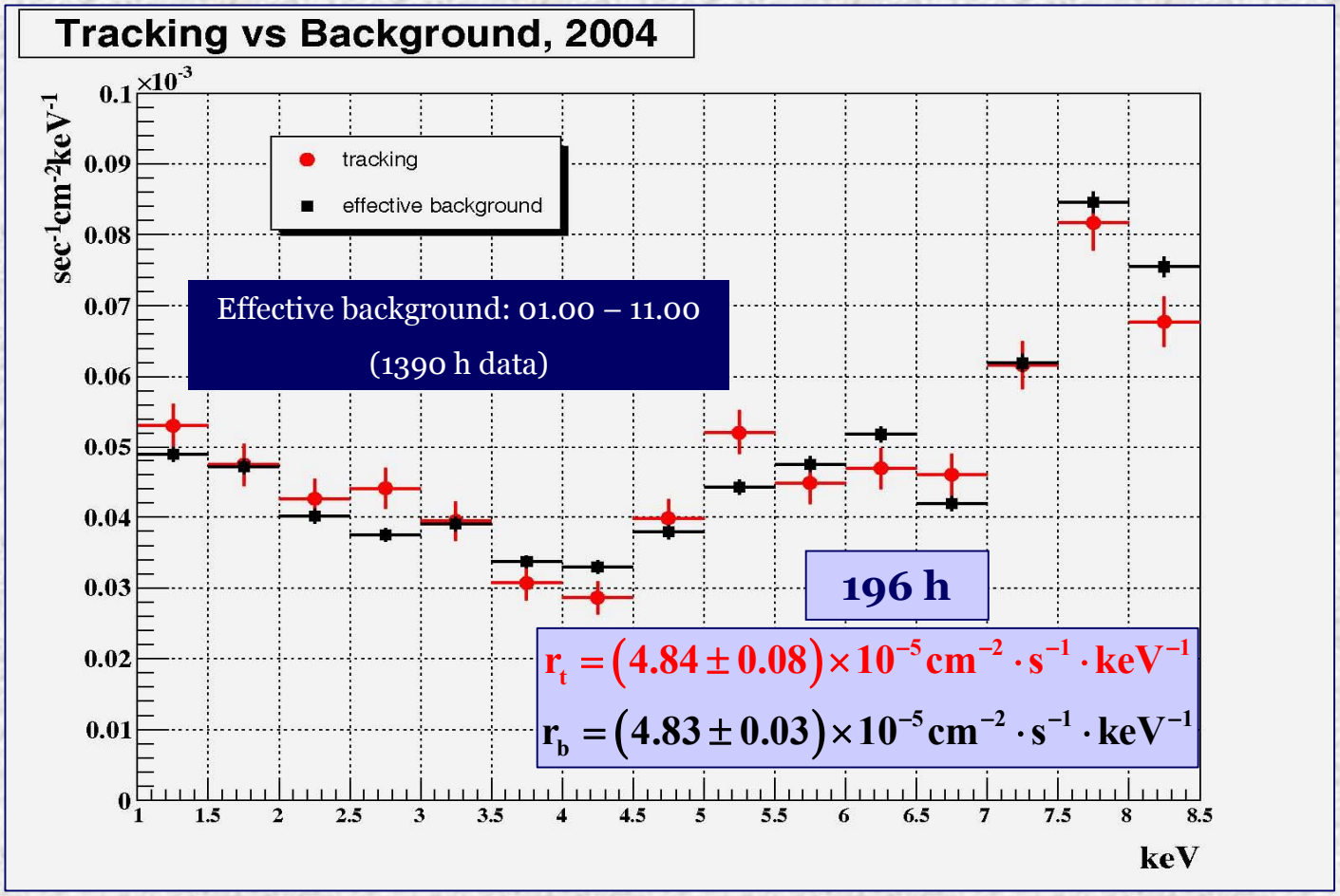
Tracking vs Background, 2004
tracking
effective background
Effective background: 01.00 – 11.00
(1390 h data)
196 h
$r_t = (4.84 \pm 0.08) \times 10^{-5} cm^{-2} \cdot s^{-1} \cdot keV^{-1}$
$r_b = (4.83 \pm 0.03) \times 10^{-5} cm^{-2} \cdot s^{-1} \cdot keV^{-1}$
$\times 10^{-3}$
$sec^{-1}cm^{-2}keV^{-1}$
keV

Calculation of an upper limit for $g_{\alpha\gamma\gamma}$

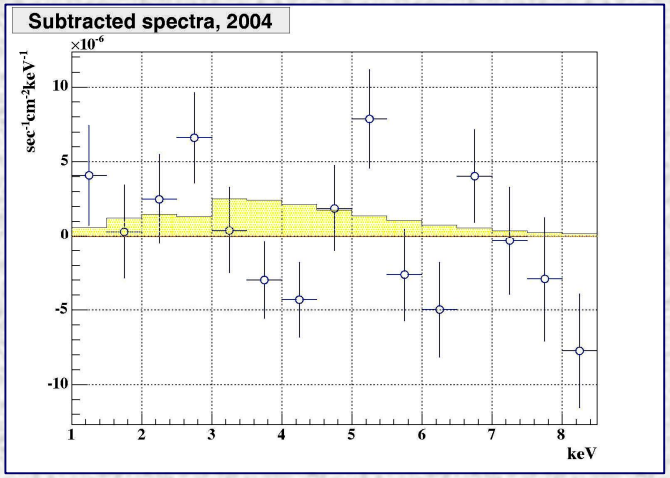

$$N_i^{\alpha} = f(E_i) \times A_m \times t \times P_{\alpha\to\gamma} \times \alpha_h(E_i) \times \alpha_s \times dE$$

$$N_i^{m} = (r_i^t - r_i^b) \times t \times dE \times A$$

$$\chi^2 = \sum_{bins} \left(\frac{N_i^{\alpha} - N_i^{m}}{\sigma_i} \right)^2$$

$$\sigma_i = \sqrt{N_i^t + \left(\frac{t_t}{t_b}\right)^2 N_i^b}$$

fitting parameter: $C = g_{10}^4$

$f(E) \sim g_{10}^2$ (axion flux)

$g_{10} = g_{\alpha\gamma\gamma} \times (10^{10}\,\mathrm{GeV})$

$A_m = 14.5\ \mathrm{cm}^2$

$t = 196$ h

$P_{\alpha\to\gamma} = 0.25 \times B^2 L^2 g_{\alpha\gamma\gamma}^2$, $m_\alpha < 0.02$eV

$\alpha_h(E)$: hardware efficiency (detection+strongback+dead time)

α_s: software efficiency

$dE = 0.5$ keV

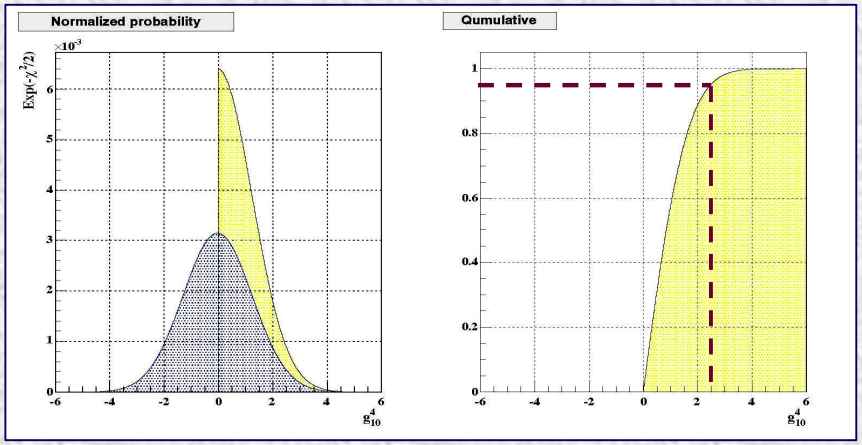

Bayes method

$$(1-a)\int_0^{+\infty} \exp\left(-\frac{\chi^2}{2}\right) dC = \int_0^{C_{up}} \exp\left(-\frac{\chi^2}{2}\right) dC$$

Degree of belief (a)

Upper limit (C_{up})

Calculation of an upper limit for $g_{\alpha\gamma\gamma}$

1 - 8.5 keV

Effective background	Best fit	χ^2_{min} / ndf	χ^2_{null} / ndf	95% CL 10^{-10} GeV^{-1}
00.00-12.00	0.21 ± 0.89	24.73 / 14	24.75 /15	1.27
01.00-11.00	-0.03 ± 0.9	26.84 /14	26.84 / 15	1.25
02.00-10.00	-0.35 ± 0.92	30.11 / 14	30.18 / 15	1.23
03.00-09.00	-0.67 ± 0.94	31.77 / 14	32.02 / 15	1.22

$$g_{\alpha\gamma\gamma} < (1.25 \pm 0.02 \pm 0.007) \times 10^{-10} \mathrm{GeV}^{-1}$$

$$m_\alpha < 0.02 \mathrm{eV}$$

1 - 7.5 keV

Effective background	Best fit	χ^2_{min} / ndf	χ^2_{null} / ndf	95% CL 10^{-10} GeV^{-1}
00.00-12.00	0.29 ± 0.9	20.83 /12	20.88 /13	1.28
01.00-11.00	0.06 ± 0.9	22.26 /12	22.26 / 13	1.26
02.00-10.00	-0.24 ± 0.92	23.93 /12	23.97 / 13	1.24
03.00-09.00	-0.55 ± 0.94	24.54 /12	24.71 / 13	1.23

Simulation of the efficiency systematics.

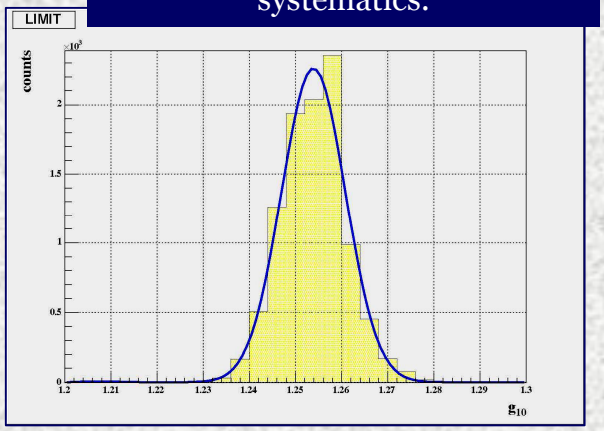

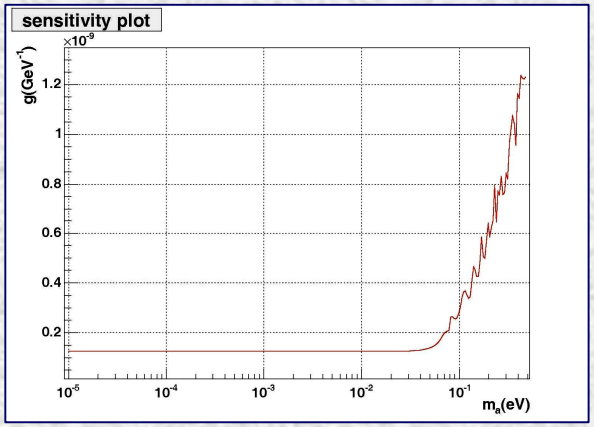

CAST results

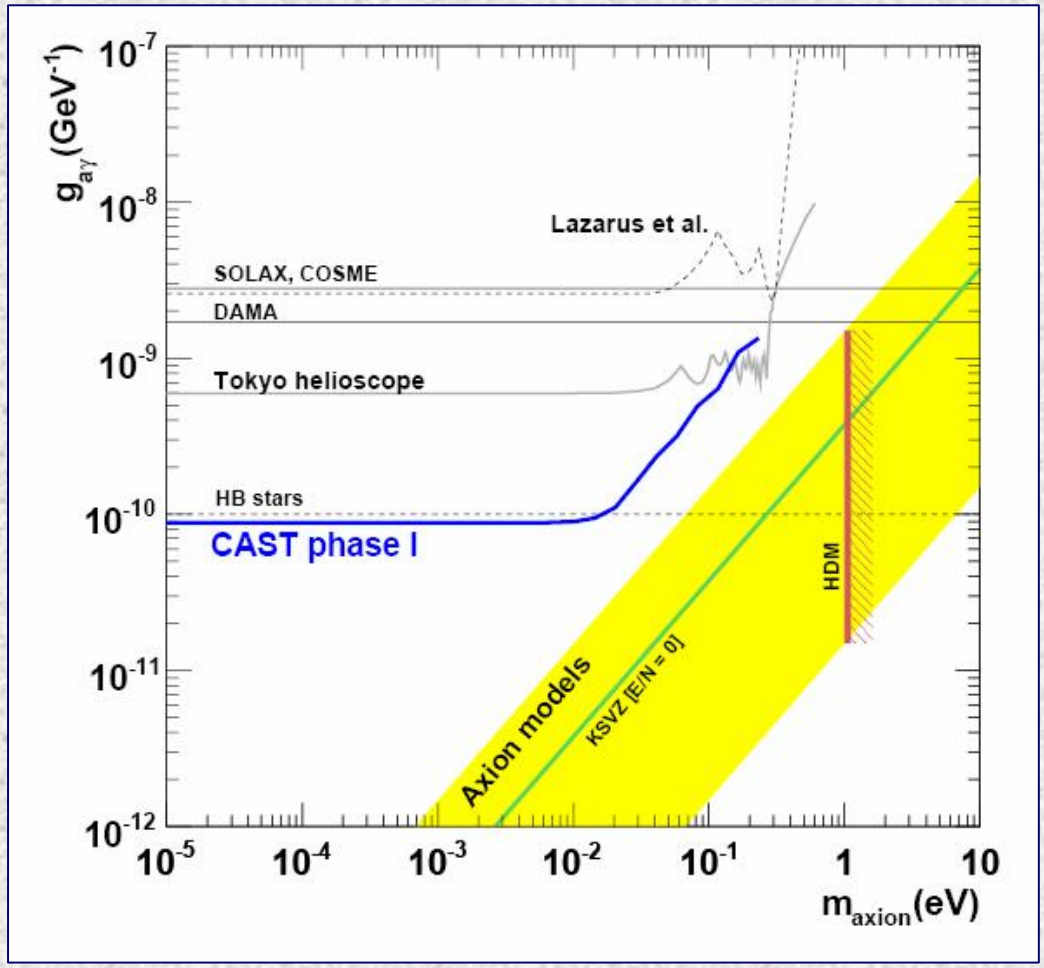

95% C.L. (Bayes) upper limt

$$g_{\alpha\gamma\gamma} < 8.8 \times 10^{-11}\,\mathrm{GeV}^{-1}$$

Submitted for publication (JCAP)

hep-ex/0702006 :

"An improved limit on the axion – photon coupling from the CAST experiment "

CAST Phase II principle

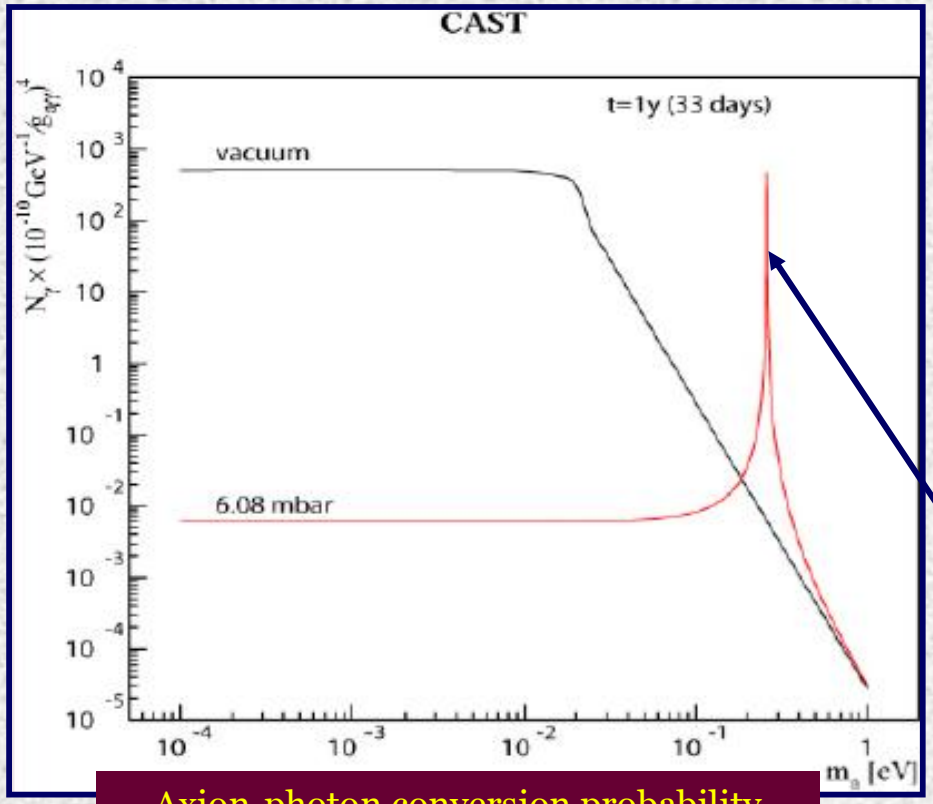

Axion-photon conversion probability

m_γ=effective photon mass

$$m_\gamma \approx \sqrt{\frac{4\pi\alpha N_e}{m_e}} = 28.9\sqrt{\frac{Z}{A}\rho} \quad \text{eV}$$

ρ=gas density (g/cm³)

$$q = \frac{\left|m_a^2 - m_\gamma^2\right|}{2E} \quad \textbf{(momentum transfer)}$$

Coherence condition:
qL<<1

CAST Phase II status & prospects

Phase II operation (^{4}He)

- Data taking with 4He performed all along 2006
- ~160 density steps performed, reaching ~13 mbar (~0.39 eV)
- Approximate explored region shown in plot
  - QCD axion models region is entered !!.
- Data now under analysis
- ^{3}He phase will start mid 2007 (upgrade works ongoing)

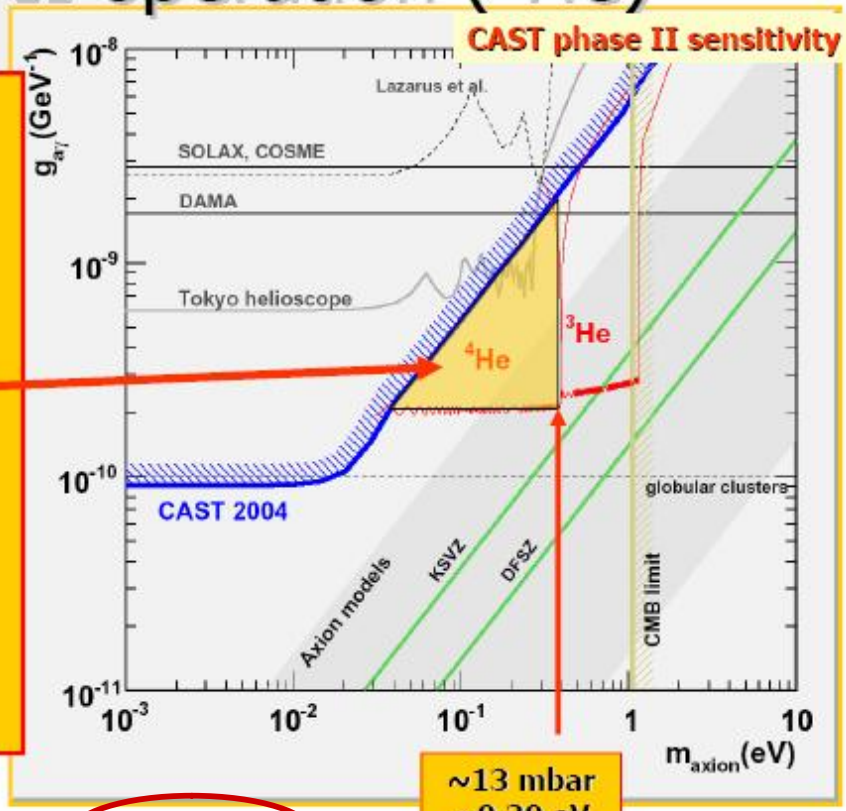

Moriond EW 2007 Igor G. Irastorza 11

Copyright: I. G. Irastorza

Conclusions

- The Strong CP problem remains unresolved for 30 years and the dynamic Peccei-Quinn solution is the most viable. Axion searches are too important to ignore.
- Following the analysis of the data collected with the Micromegas detector during CAST Phase I **there is no axion signal**.
- The missing axion signal leads to the calculation of an upper limit for the axion-photon coupling constant which improves the limits from previous experiments by a factor ~7.
- CAST continues with Phase II, entering unexplored regions of the axion parametric space.
- The Micromegas detector is a stable and reliable structure, as proved by its performance in the CAST experiment.

- The 2003 data were used mostly for the understanding of the detector, while the 2004 data were used to make Physics analysis.
- The spectrum of the measured background from the Micromegas detector is fully understood, with the aid of the simulation and it comes from the fluorescence of its constructing materials.
- The multivariate analysis is more suitable when the event selection rules are based on correlated discriminant quantities.
- The dominant systematical error is the diurnal variation of the measured background and it was taken into account by defining an effective background. The total effect of the systematical errors to the calculated upper limit of the axion–photon coupling constant is less than 2%.

Presentations

Publications

1. Performance of the Micromegas detector in the CAST experiment, **Nucl.Instrum.Meth.A573:38**, 2007
2. First results from the CERN Axion Solar Telescope (CAST), **Phys.Rev.Lett.94:121301**, 2005.
3. A low background Micromegas detector for axion searches, **Nucl.Instrum.Meth.A535:309**, 2004.
4. The use of the Micromegas technology for a new imaging system, **Nucl.Instrum.Meth.A527:62**,2004.
5. An improved limit on the axion-photon coupling from the CAST experiment, **Submitted to JCAP.**
6. The Micromegas detector of the CAST experiment, **Submitted to New J. Phys.**

Conferences

1. HEP2004, Chios.
2. PSD7 2005, Liverpool.
3. HEP2006, Ioannina.

CAST collaboration meetings

1. 17th Col.Meeting (2003-CERN).
2. 23rd Col.Meeting (2004-Munich).
3. 24th Col.Meeting (2005-CERN).
4. 25th Col.Meeting (2005-CERN).
5. 27th Col.Meeting (2005-CERN).
6. 28th Col.Meeting (2006-Zaragoza).

Acknowledgements

G. Fanourakis T. Geralis K. Zachariadou	**NCSR "Demokritos"**
I. Giomataris E. Ferrer Ribas S. Aune	**Saclay**
K. Zioutas T. Papaevangelou I. G. Irastorza T. Dafni B. Lakic	**CAST**

BACKUP

Micromegas

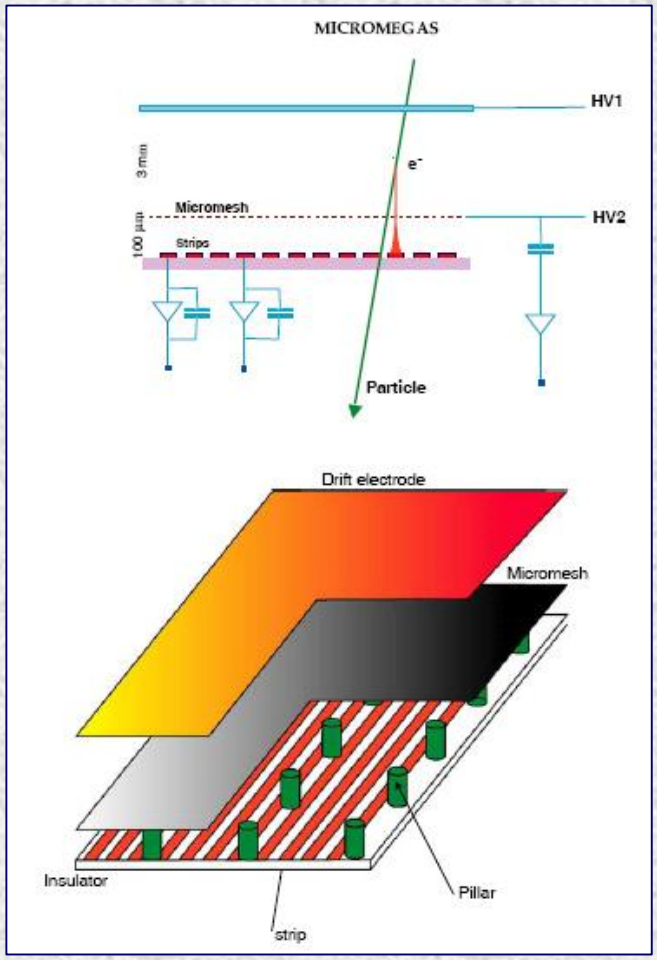

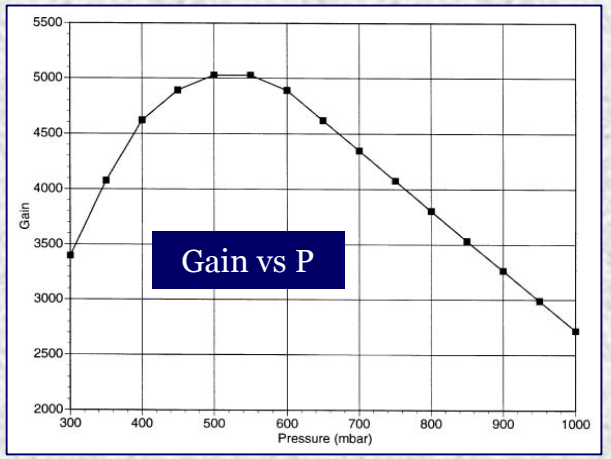

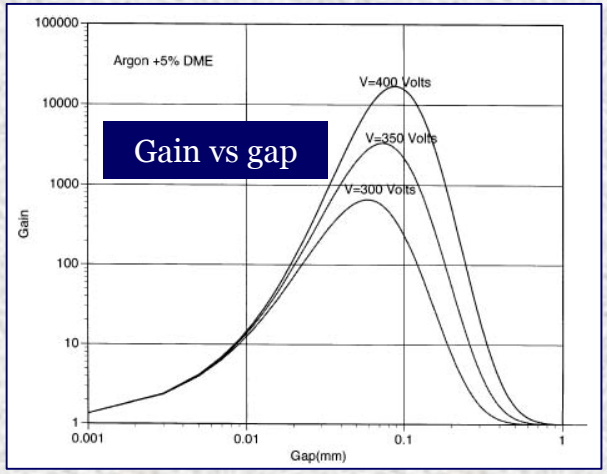

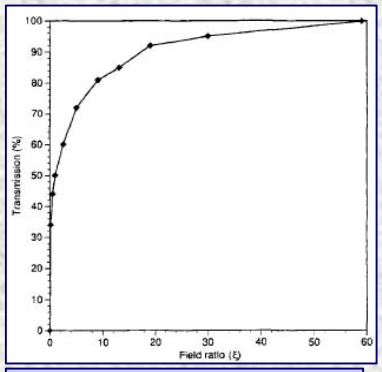

$$M = e^{\alpha \cdot d}$$

$$\alpha = p \cdot A \cdot \exp\left(-C\frac{pd}{V}\right)$$

(Rose & Korff)

$$\frac{\delta M}{M} = \alpha \cdot d \cdot \left(1 - \frac{Cpd}{V}\right) \cdot \frac{\delta d}{d}$$

- α: Townsend coefficient.
- d: amplification gap.
- V: High voltage.
- p: gas pressure.
- A,C: gas constants.

Pulse analysis

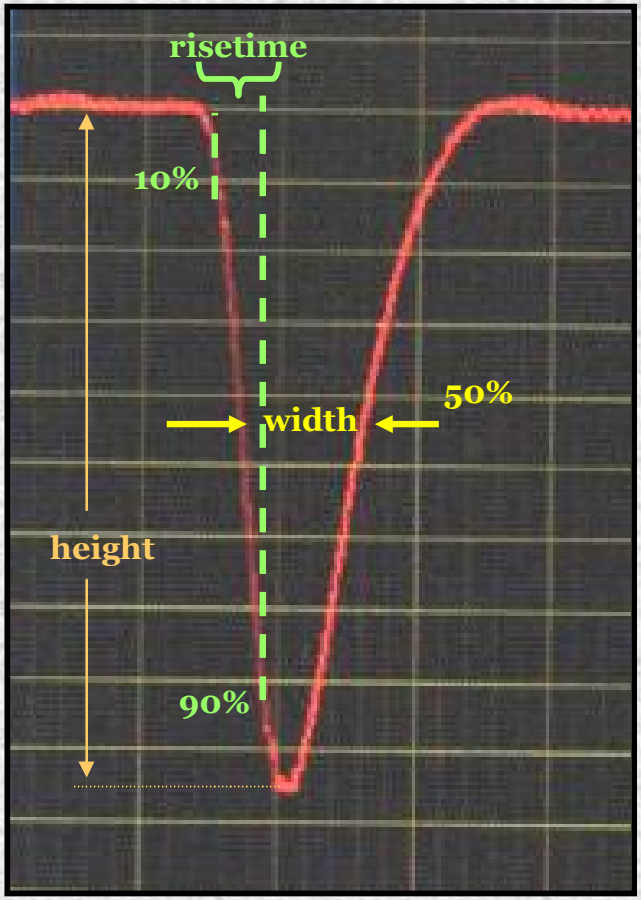

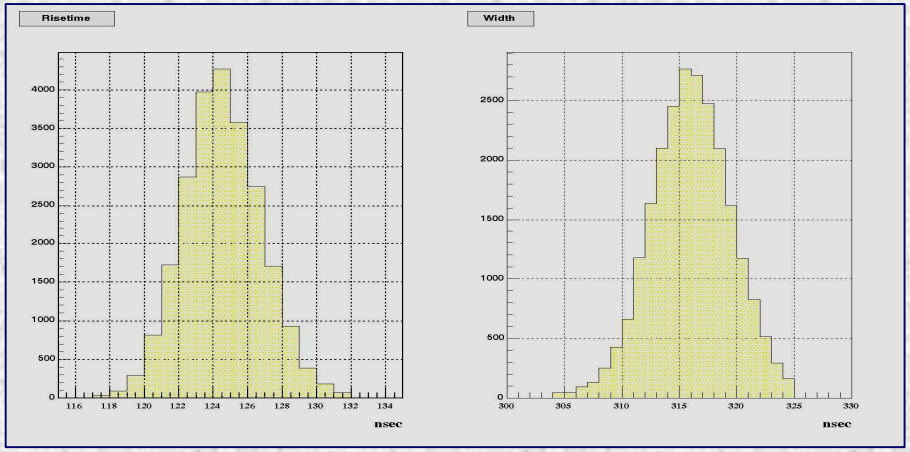

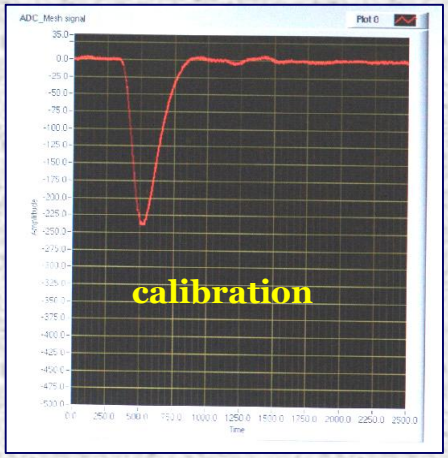

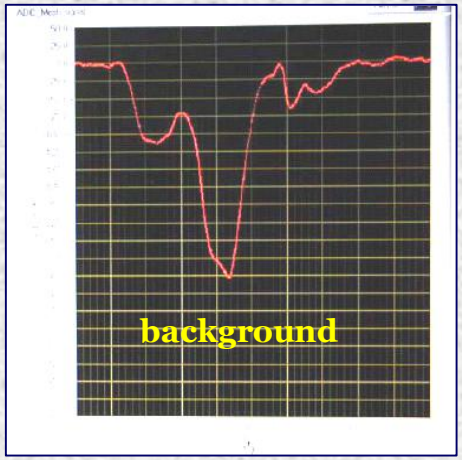

Typical strip data

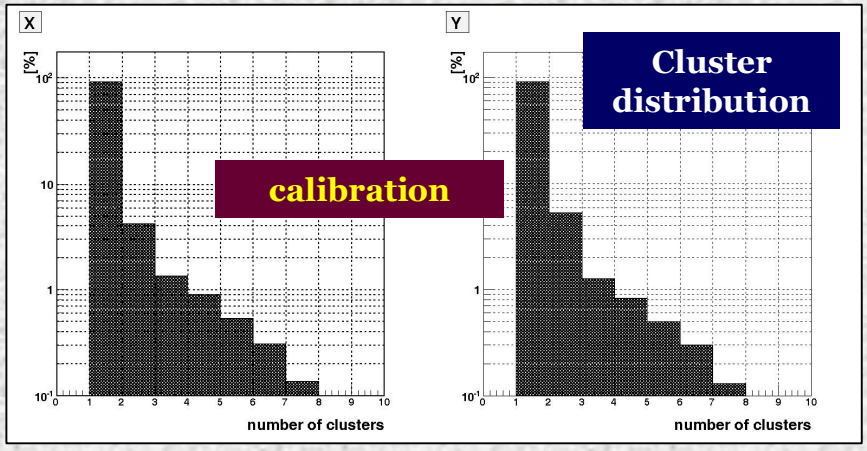

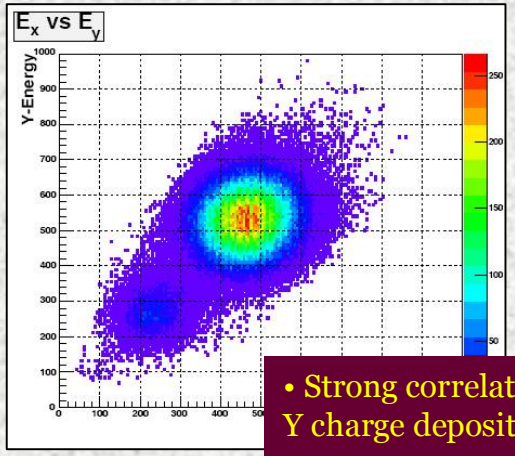

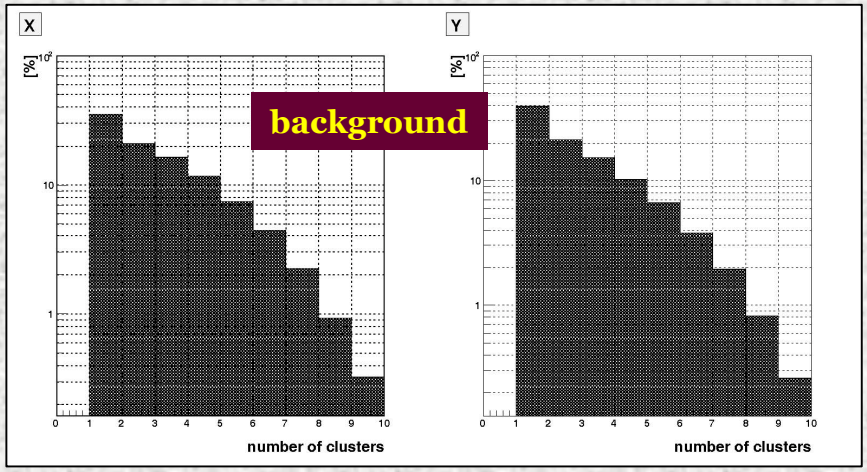

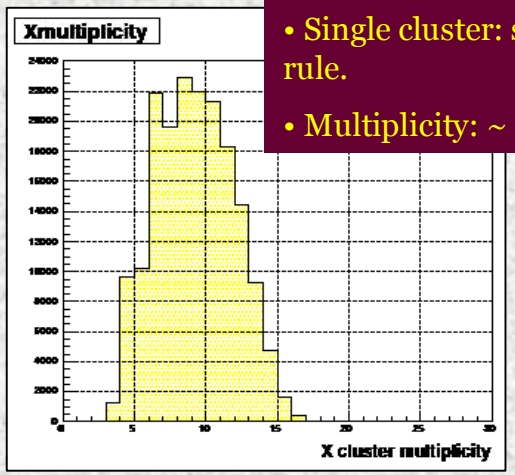

- Strong correlation between X and Y charge deposition.
- Single cluster: strong selection rule.
- Multiplicity: ~ 9 strips/cluster.

Data processing

DAQ

Run Number

mmRxxxx.dat

- Run header
  - Event header
    - Event body
  - Event footer
  - *More events……*
- Run footer

- **X-Y Clustering** (number of clusters, multiplicity, charge, barycenter).
- **Event reconstruction** (identification through total charge).
- **Pulse processing** (center, risetime, width, height, integral).

mmRxxxx.clu

Final event selection

Effect of gas density variation on the detector efficiency

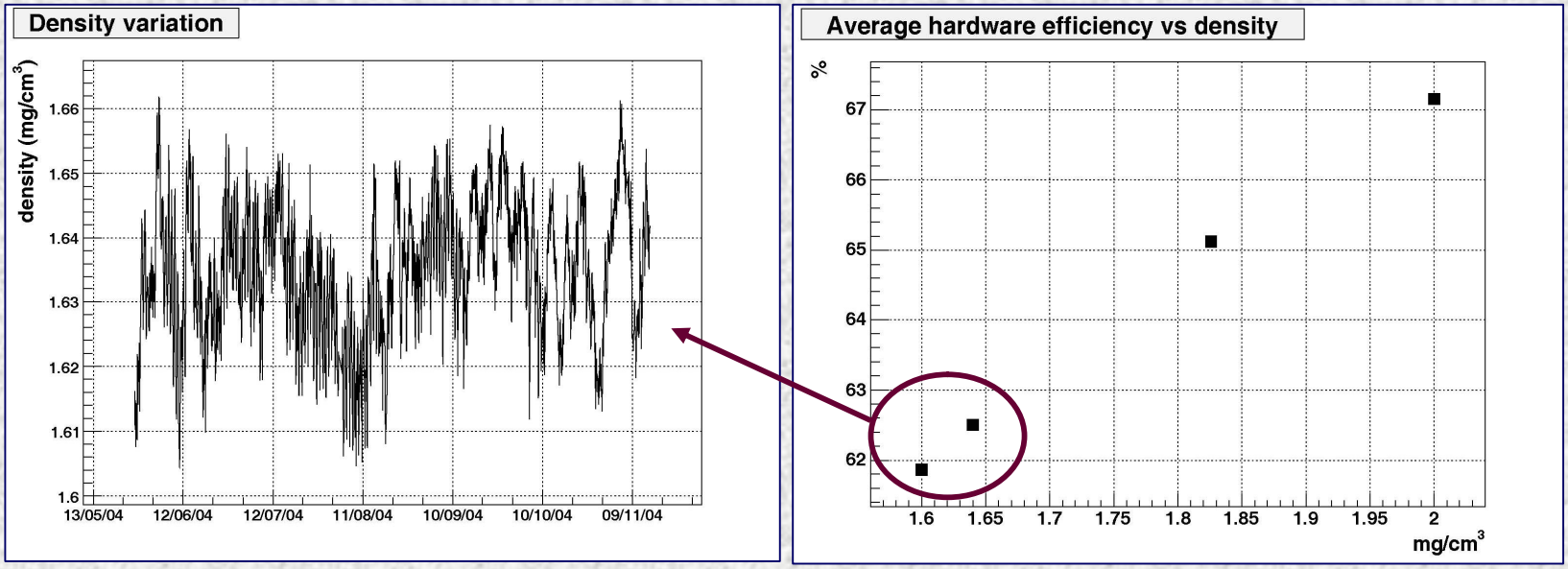

Solar axions

Primakoff effect

$$\frac{d\sigma_{\alpha\leftrightarrow\gamma}}{d\Omega} = \frac{g_{\alpha\gamma\gamma}^2 Z^2 e^2}{32\pi^2} \frac{\left|\vec{p}_\alpha \times \vec{p}_\gamma\right|^2}{\left|\vec{p}_\alpha - \vec{p}_\gamma\right|^4}$$

Charge screening

$$V(r) = \frac{Ze}{4\pi} \cdot \frac{e^{-\kappa_s r}}{r}$$

$$x = \frac{r}{R_\odot}$$

$$\omega_p = \sqrt{\frac{4\pi\alpha_{em} n_e}{m_e}}$$

$$E^2 = k^2 + \omega_p^2$$

$$f_B = \frac{1}{e^{E/T} - 1}$$

$$\kappa_s^2 = \frac{4\pi\alpha_{em}}{T}\left(n_e + \sum_{\text{nuclei}} Z_j^2 n_j\right)$$

$$\frac{1}{\kappa_s} = \text{Debye-Huckel screening length}$$

$$\Gamma_{\gamma\to\alpha} = \frac{g_{\alpha\gamma\gamma}^2}{32\pi} \cdot T \cdot \kappa_s^2 \cdot \left[\left(1 + \frac{\kappa_s^2}{4E^2}\right) \cdot \ln\left(1 + \frac{4E^2}{\kappa_s^2}\right) - 1\right]$$

Axion luminosity

$$L_\alpha = 2R_\odot^3 \int_0^1 dx \cdot 4\pi x^2 \int_{\omega_p}^\infty dE \frac{4\pi k^2}{(2\pi)^3} \cdot \frac{dk}{dE} \cdot E \cdot f_B \cdot \Gamma_{\gamma\to\alpha}$$

Axion flux on Earth

$$\Phi_{\bar{\alpha}} = \frac{R_\odot^3}{\pi^2 D_\oplus^2} \int_0^1 dx \cdot x^2 \int_{\omega_p}^\infty dE \cdot k \cdot f_B \cdot \Gamma_{\gamma\to\alpha}$$

Alignment to the Sun

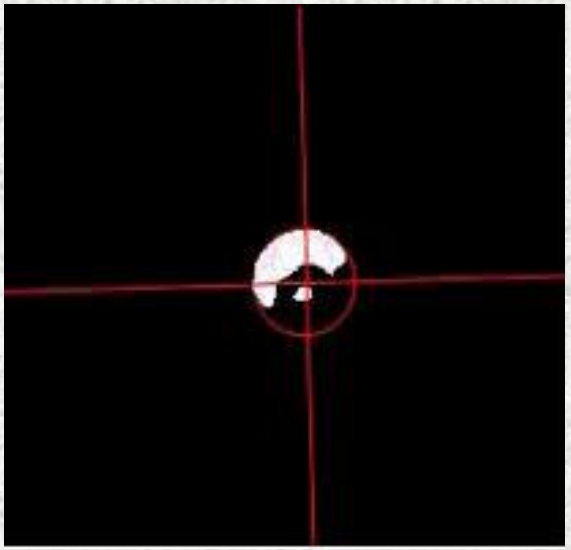

March 2003

Stability

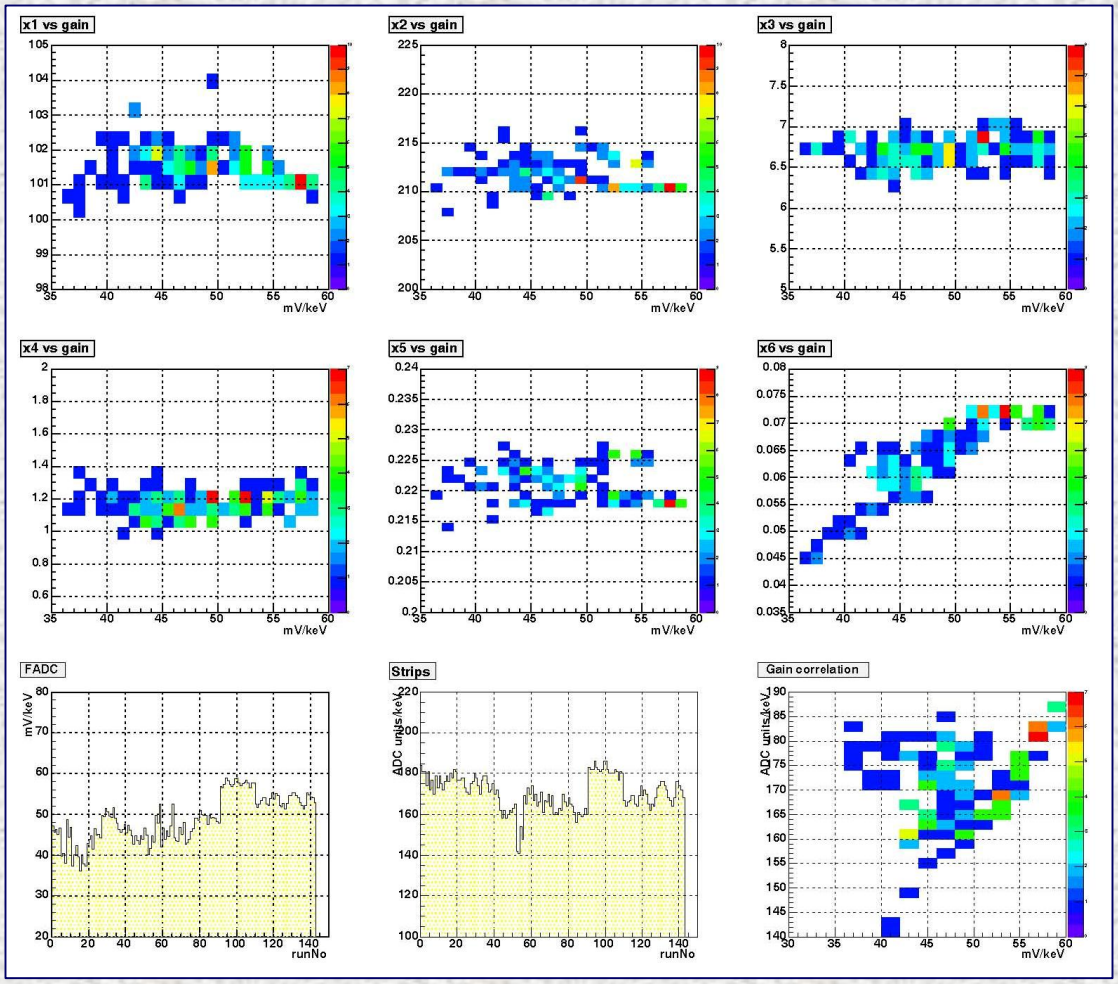
x1 vs gain
x2 vs gain
x3 vs gain
x4 vs gain
x5 vs gain
x6 vs gain
mV/keV
FADC
Strips
Gain correlation
runNo
ADC units/keV

Booh!

Stability

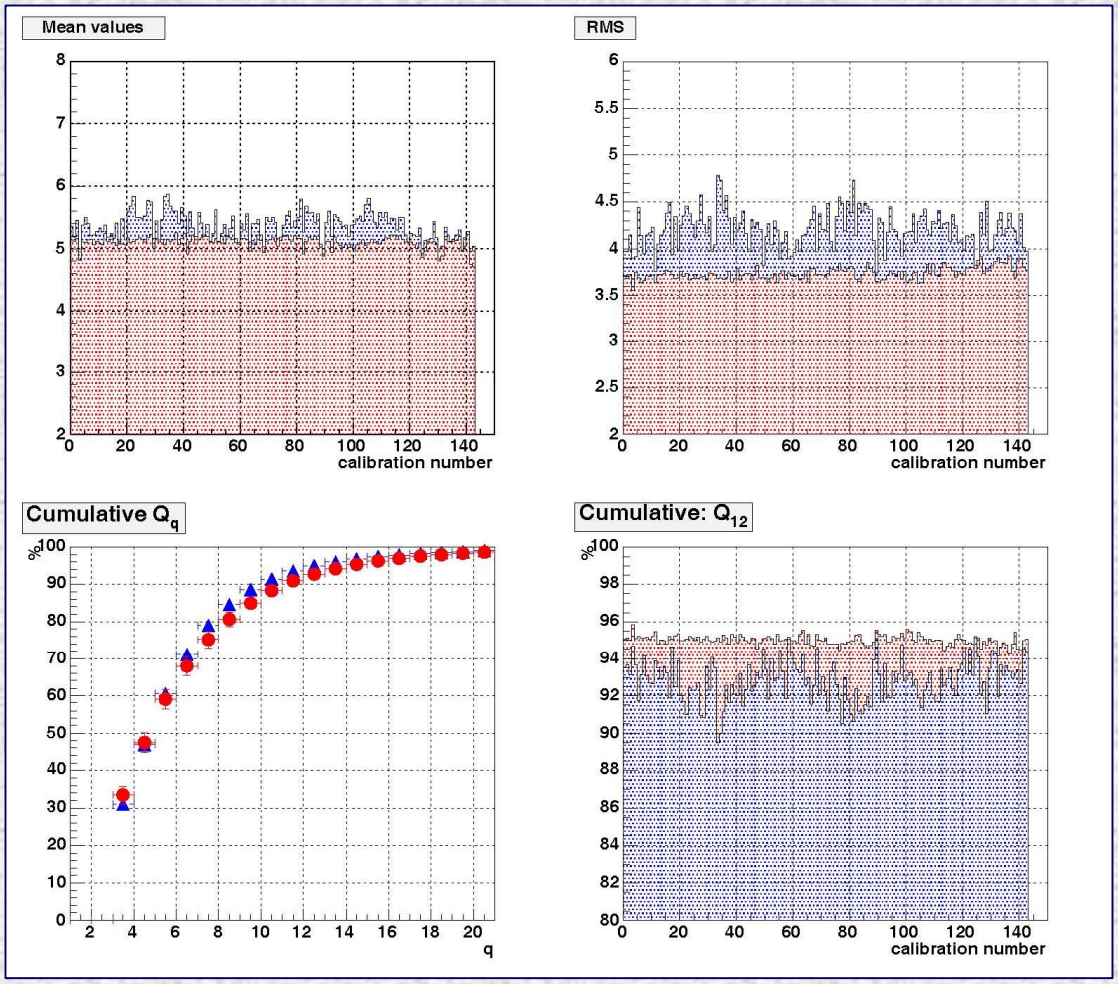
Mean values
calibration number
RMS
calibration number
Cumulative Q_q
%
q
Cumulative: Q_{12}
%
calibration number